

**SYNTHESIS,
CHARACTERIZATIONS AND
APPLICATIONS OF CARBON
DOTS (CDs) and Au-COATED
CARBON DOTs (AuCDs)**



NUST
NATIONAL UNIVERSITY
OF SCIENCES & TECHNOLOGY

Habiba Anjum

Fall 2020-MS Physics

Reg. No.: 00000330850

Research Supervisor

Dr. Faheem Amin

Department of Physics

School of Natural Sciences (SNS)

National University of Sciences and Technology (NUST)

H-12 Islamabad, Pakistan.


THESIS ACCEPTANCE CERTIFICATE

Certified that final copy of MS thesis written by **Habiba Anjum** (Registration No. **00000330850**), of **School of Natural Sciences** has been vetted by undersigned, found complete in all respects as per NUST statutes/regulations, is free of plagiarism, errors, and mistakes and is accepted as partial fulfillment for award of MS/M.Phil degree. It is further certified that necessary amendments as pointed out by GEC members and external examiner of the scholar have also been incorporated in the said thesis.

Signature:  _____

Name of Supervisor: Dr. Faheem Amin

Date: _____

Signature (HoD):  _____

Date: 21-12-2023

Signature (Dean/Principal):  _____

Date: 21.12.2023

National University of Sciences & Technology

MS THESIS WORK

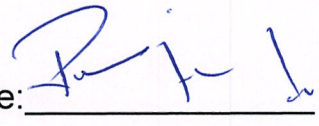
We hereby recommend that the dissertation prepared under our supervision by: Habiba Anjum, Regn No. 00000330850 Titled: "Synthesis, Characterisations and Applications of Carbon Dots (CDs) and Au Coated Carbon Dots (AuCDs)" accepted in partial fulfillment of the requirements for the award of **MS** degree.

Examination Committee Members

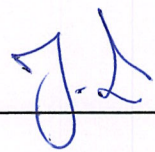
1. Name: PROF. SYED RIZWAN HUSSAIN

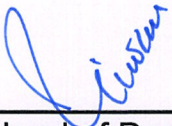
Signature: 

2. Name: DR. RUMEZA HANIF

Signature: 

Supervisor's Name: DR. FAHEEM AMIN

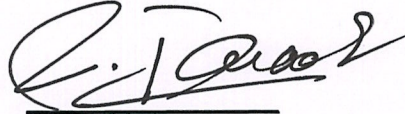
Signature: 


Head of Department

21-12-2023
Date

COUNTERSIGNED

Date: 21.12.2023


Dean/Principal

DEDICATION

**I dedicate my research work to my whole family, especially to my parents,
For their persistent support, love, and encouragement.**

ACKNOWLEDGEMENT

Praise and glory belong to **Allah Almighty** whose Throne extends over all that exists by His grace. Alhamdulillah for everything I had and Alhamdulillah for everything I will have.

It's an honor to acknowledge all those who have supported me throughout the research. I am extremely grateful to my beloved parents for their unconditional love and support throughout my life.

The thesis would be incomplete without being thankful for the guidance, and meticulous attention, given to me by my supervisor **Dr. Faheem Amin** throughout the course of this research project. There is compassion in the way he teaches and the way he supervises. Your guidance, mentoring, and teaching have improved me in every walk of life. Everything done under this project is owed to him.

I would like to express my gratitude to the Rector NUST, Principal SNS **Prof. Rashid Farooq**, and Head of the Department of Physics **Prof. Syed Rizwan Hussain** for providing me with the opportunity to complete my MS Physics degree here at SNS.

I would like to extend a special acknowledgment for the guidance and assistance provided to me by my GEC members **Prof. Syed Rizwan Hussain** and **Dr. Rumeza Hanif**. I am utterly thankful to all the teachers I had throughout my life for shaping my personality in a way that allowed me to reach the level I am at today.

Finally, all my prayers and obligations towards my family, especially my parents, I will always be indebted.

ABSTRACT

In current research, Carbon dots (CDs) and Au-coated Carbon dots (AuCDs) have been synthesized using Hydrothermal and conventional coating methods. AuCDs are a novel candidate in nanomaterials. Different characterization techniques, for instance; UV-visible spectroscopy, Fluorescence spectroscopy, XRD, FTIR, SEM, and EDX have been utilized to investigate the optical, morphological, structural, and elemental characteristics of CDs and AuCDs. UV-visible spectroscopy, SEM, and EDX confirm the Au coating on the surface of CDs. UV-visible spectroscopy depicts the SPR band and broad CDs peak on Au coating. FTIR shows the existence of -OH and-COOH on CDs' surface which aids in the formation of AuCDs. Electrochemical biosensing of Glucose proves the excellent sensitivity, electrical conductivity, and catalytic activity of CDs and AuCDs. Optical detection of metal ions confirms the ability of CDs to be used as Optical sensors for Cu ion detection. Cytotoxicity assessment on HEK-293T and MDA-MB-231 depicts that at higher concentrations, CDs and AuCDs have higher toxicity and are almost non-toxic at lower concentrations. Also, AuCDs show a higher level of toxicity as compared to CDs. Thus, CDs can be utilized for the sake of Electrochemical biosensing, Optical detection, and Cancer therapy. In addition, AuCDs act as a novel contribution in the field of nanoparticles that can be utilized in the fields of Electrochemical biosensing, Optical detectors, and Theranostic agents.

KEYWORDS: Carbon dots (CDs), Au-coated Carbon dots (AuCDs), Electrochemical biosensing, Glucose, Optical detection, Cytotoxicity.

TABLE OF CONTENTS

DEDICATION	I
ACKNOWLEDGEMENT	II
ABSTRACT.....	III
LIST OF FIGURES	VII
Chapter 1	1
INTRODUCTION	1
1.1. Introduction to Carbon Dots (CDs)	2
1.2. Applications of Carbon Dots	6
1.3. Introduction of Gold Nanoparticles	8
1.4. Applications of Gold Nanoparticles	10
1.5. Gold Coated Carbon Dots (AuCDs).....	13
1.6. Aims and Scope	13
1.7. Objectives of the Study.....	14
Chapter 2.....	15
LITERATURE REVIEW	15
2.1. Optical Detection of Metal Ions	15
2.2. Electrochemical Biosensing of Glucose	16
2.3. Cytotoxicity Assessment	17
Chapter 3.....	20
METHODOLOGY AND CHARACTERIZATION TECHNIQUES	20
3.1. Chemical Reagents	20
3.2. Synthesis of Carbon Dots	20
3.2.1. Hydrothermal Carbonization.....	21
3.2.2. Synthesis Reaction	21
3.3. Synthesis of Au-Coated Carbon Dots (AuCDs)	22
3.4. Characterization of CDs and AuCDs.....	22
3.4.1. X-Ray Diffraction (XRD)	23
Components of X-ray Diffractometer	23

Fundamental Principle of X-ray Diffraction.....	24
3.4.2. Ultraviolet Visible (UV-Vis) Spectroscopy	25
Fundamental Principle of UV-Vis Spectrophotometer.....	25
3.4.3. Scanning Electron Microscopy (SEM)	26
Components of SEM.....	26
Fundamental Principle of SEM.....	27
3.4.4. Energy Dispersive X-Ray Spectroscopy (EDX).....	28
3.4.5. Fourier Transform Infrared Spectroscopy (FTIR)	29
Working Principal of FTIR.....	29
3.4.6. Potentiostat.....	30
Configuration of Potentiostat.....	31
3.4.6.1. Cyclic Voltammetry (CV).....	32
Fabrication of Working Electrode	32
3.4.7. Cytotoxicity Assessment.....	33
Culturing of Cell Lines	33
Subculturing of Cell Lines	33
NPs Dilutions and Plating.....	34
MTT Assay	34
Calculation of Cell Survival and Cell Inhibition Percentage.....	35
Chapter 04.....	36
RESULTS AND DISCUSSIONS.....	36
4.1. UV-Visible Spectroscopy	36
4.2. Scanning Electron Microscopy (SEM).....	36
4.3. Energy Dispersive X-ray Spectroscopy (EDX).....	37
4.4. X-Ray Diffraction.....	38
4.5. Fourier Transform Infrared Spectroscopy	39
4.6. Electrochemical Measurements.....	40
Glucose Detection Via Electrochemical Sensing.....	40
4.7. Optical Detection of Metal Ions	42
4.8. Cytotoxicity Assessment	44

Chapter 5.....	47
CONCLUSION AND FUTURE RECOMMENDATIONS	47
Future Recommendations	48
REFERENCES	49

LIST OF FIGURES

Figure 1: Overall Structure of Carbon Dots (Jorns & Pappas, 2021).....	3
Figure 2: Schematic Description of the Diverse Methods for Carbon Dots Synthesis (De & Karak, 2017).....	4
Figure 3: Gold Nanoparticles' Desirable Characteristics (Patil et al., 2023)	9
Figure 4: Synthesis, Assembly and Storage Process of Carbon Dots.....	21
Figure 5: Synthesis, Assembly and Storage Process of Carbon Dots.....	22
Figure 6: X-ray Diffractometer (Despotopoulou, 2019).....	24
Figure 7: Bragg's Law Schematic (Venkata Sivareddy, Krishna, & Venu Gopal, 2022).....	25
Figure 8: UV-Visible Spectrophotometer (Rocha, Gomes, Lunardi, Kaliaguine, & Patience, 2018)	26
Figure 9: Schematic Diagram of SEM (Ananthapadmanaban, 2018).....	27
Figure 10: Working Principal of SEM (Ezzahmouly et al., 2019).....	28
Figure 11: Working Principal of EDX (Long, Nand, & Ray, 2021).....	29
Figure 12: Schematic Working of FTIR (S. K. Rahi, Hassan, & Abd, 2016)	30
Figure 13: Color Scheme of 3-electrode setup	31
Figure 14: Schematic of an electrochemical cell.....	32
Figure 15: MTT Assay Protocol	35
Figure 16: UV-Visible Spectra of Carbon Dots, and AuCDs	36
Figure 17: SEM images of core/shell nanoparticles A) Carbon Dots B) AuCDs	37
Figure 18: EDS Spectra and corresponding Elemental Composition of A) Carbon Dots B) AuCDs.....	38
Figure 19: XRD Pattern of Carbon Dots and AuCDs	39
Figure 20: FTIR Spectra of Carbon Dots and AuCDs	40
Figure 21: Electrochemical Sensing of Glucose using 0.1M NaOH as electrolyte through A) Carbon Dots B) AuCDs	42
Figure 22: Optical Detection of Metal Ions Via A) CDs at pH3 B) CDs at pH8 C) CDs at pH5 D) AuCDs at pH5	44
Figure 23: Cytotoxicity Assessment on HEK-293T and MDA-MB-231 Cell Lines via Carbon Dots and AuCDs.....	46

Chapter 1

INTRODUCTION

Nanotechnology, also known as 1 nm to 100 nm (10^{-9} m) scale manipulation, is the process of altering the dimensions and shape of structures, electronics, and systems. The Greek word "nano" (which referring to "very small") is the origin of the prefix "nano" for the unit of nanometer. A global non-governmental organization of national standards bodies ISO (International Organization for Standardization), defines nanoparticles as nano-objects having all of their external dimensions in the nanoscale, where the longest and shortest axes' dimensions do not differ considerably. (80004-2:, 2015).

Due to their small size, they exhibit greater reactivity, more significant surface areas than the analogous bulk forms, and a variety of characteristics that can be altered (Salem, Hammad, Mohamed, & El-DougDoug, 2022). The length of a nanometer can be visualized as five silicon atoms or ten hydrogen atoms queued up. Richard Adolf Zsigmondy initially coined the word "nanometer" in 1914. The notion of "nanotechnology" was introduced pioneered in a speech delivered at the annual meeting of the American Physical Society in 1959 by the American scientists and the Nobel Prize laureate Richard Feynman. This is regarded as the first academic lecture on nanotechnology. "There's Plenty of Room at the Bottom" was title of the lecture delivered by him (Feynman, 1960). In 1974, Norio Taniguchi may be credited as the first to use the notion "nanotechnology". Nanotechnology, according to Norio Taniguchi, primarily refers to single atom or molecule's treatment, separation, reorganization, and transformation of a material (Taniguchi, 1974).

NPs are composed of three distinct layers since they aren't simple molecules: (a) the surface layer, which can be functionalized with a wide range of surfactants, small particles, and polymeric materials; (b) the shell layer, which is a material that is chemically distinct from the core in each aspect; and (c) the core, which is the central region of the NP and usually corresponds to the NP itself. (Khan, Saeed, & Khan, 2019).

The dimensions, topography, structure, size, and manufacturing techniques of nanoparticles all have the potential to classify them. However, nanomaterials are often classified using their morphology, composition, uniformity, agglomeration, and dimensionality. The classification of nanoparticles based on morphology takes into account the aspect ratio, geometry, and flatness. Nanoparticles are divided into oval, cubical, tetrahedron-shaped, spherical, pillar-like, and colloidal categories on the basis of their low aspect ratio. While nanoparticles can be categorized as nano-rods, nano-stars, nano-springs, nano-hooks, nano-helices, and nano-plates because of their high aspect ratio. Based on dimensionality, nanoparticles are divided into four categories: zero-dimensional (0D), where height, breadth, and length are constrained to a singular point; one-dimensional (1D), where only a single parameter is present, either length or breadth; two-dimensional (2D), where only two parameters—length or breadth or height—are present; and three-dimensional (3D), where all three parameters—length, breadth, and height—are present. Nanoparticles can exist as uniform aerosols or agglomerates depending on their state of uniformity and agglomeration. This categorization is based on the electromagnetic characteristics of the substances, including chemistry, surface charge, and magnetism (Asha & Narain, 2020).

1.1. Introduction to Carbon Dots (CDs)

Carbon dots (CDs), with their unique characteristics and applications, serve as one of the most valuable gifts of nanotechnology. Typically, CDs are carbon nanoparticles, and less than 10 nm is the average diameter of the majority of the particles. The fact that such materials are quite stable in aqueous media and are derived out of organic compounds is highly significant from a biological perspective.

Since its initial report by Xu et al. (2004), who used the arc discharge method to synthesize single-walled carbon nanotubes (CNTs) and unintentionally came across carbon dots (CDs) as an addition of the carbon family (X. Xu et al., 2004), carbon-based nanostructures have been widely recognized by researchers in the domain of material science. Because it permanently changed the widely held belief that carbon is a black material devoid of emitting light, the capacity of CDs to fluoresce is significant. Two years later, in 2006, Sun et al. synthesized the first stable photoluminescent CNPs of multiple sizes. They called the resulting particles "carbon quantum dots (CQDs)" (Sun et al., 2006).

The basic building blocks of CDs are hydrogen and oxygen, which are evident in various ratios in addition to the carbon skeleton. They generally appear as amorphous, spherical materials composed of quasi-0D carbon and comprise less than 10 nm-diameter hybridized carbon atoms with both sp² and sp³ hybridization. Graphene quantum dots (GQDs) are distinct from CDs since they are made entirely of sp² hybridized carbon placed into a 2-dimensional honeycomb lattice. When synthesizing CDs, a variety of carbon-based materials evolve via different precursors and synthesis methods (Jorns & Pappas, 2021).

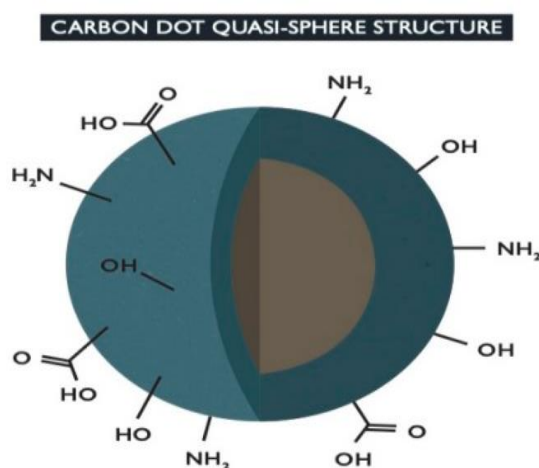


Figure 1: Overall Structure of Carbon Dots (Jorns & Pappas, 2021)

Because of their exceptional and configurable photoluminescence (PL), enhanced quantum yield (QY), non-toxic nature, compact size, impressive biocompatibility, simplicity of synthesis, electron donor and acceptor capabilities and excellent biological, physical, and chemical properties; A novel emerging star within the carbon family, carbon dots (CDs), have sparked a lot of interest. The applications encompass optoelectronic devices, biomedicine, catalysis, and anticounterfeiting. Additionally, CDs possess strong chemical stability, photobleaching resistance, excellent water solubility, and massive production (J. Liu, Li, & Yang, 2020). Additionally, they have the ease of functionalizing their surfaces with carbonyl, amino, carboxyl, hydroxyl, and epoxy groups, presenting additional perks for binding with both organic and inorganic moieties. As a result of the functionalities, CD surfaces can adopt either a hydrophilic or a hydrophobic nature, which ultimately enables the requisite thermodynamic stability in various solvents, particularly water. An effective alteration to their

properties is apparent in the CDs' surface modification via multiple functionalities, such as passivating agent and solvent (C. Ding, Zhu, & Tian, 2014).

CDs can be synthesized using a broad range of methodologies, from chemical or conventional methods to more modern biological or environmentally friendly methods, maximizing the possibility of being able to find one that is effective in multiple distinct research entities (Sivasankarapillai et al., 2020).

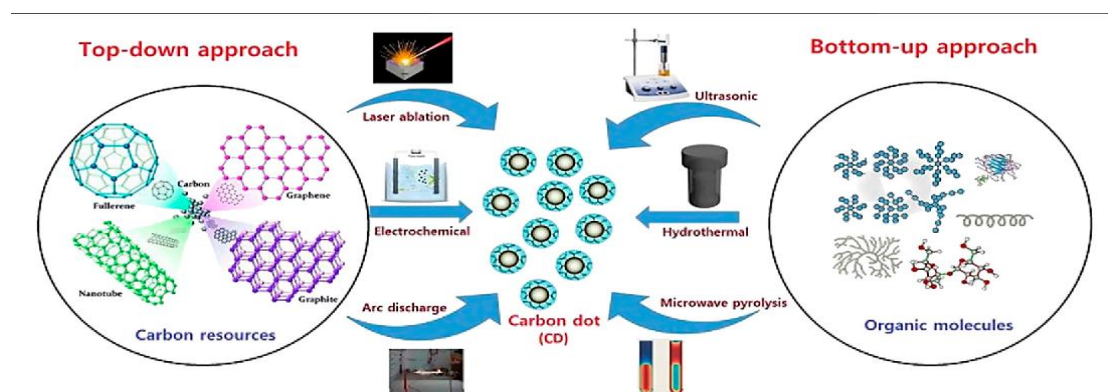


Figure 2: Schematic Description of the Diverse Methods for Carbon Dots Synthesis
(De & Karak, 2017)

In electrochemical synthesis, an electrode is employed to apply an electric potential once carbon precursors have been dissolved in a solvent. CDs form as a result of carbonization that takes place at the electrode surface (Deng et al., 2014). In arc discharge synthesis, two carbon electrodes are subjected to a high current in an inert gas environment. CDs originate in the arc as a result of vaporization caused by the extreme heat produced (Chao-Mujica et al., 2021). In laser ablation, a solid carbon material is evaporated with a high-power laser. This procedure yields a CD-containing plume of vaporized material. After that, the dots are extracted (Nguyen, Yan, Xu, & Yue, 2018). In the process of ultrasonic synthesis, carbon precursor solutions are treated with ultrasonic waves. Through a breakdown of chemical bonds and reactions brought on by cavitation, the high-intensity ultrasound radiation causes CDs formation (J. Xu et al., 2022). Pyrolysis is the process of heating organic precursors to high temperatures, usually without oxygen. As a result, the precursor material gets carbonized and CDs are generated (Romero et al., 2021). In hydrothermal synthesis, reaction solutions and carbon precursors are heated to high pressures and temperatures—typically above

100°C—in an enclosed container. This facilitates the solution's carbonization and passivation processes, which lead to the formation of Carbon dots (Ye et al., 2020). The hydrothermal method is one of the most frequently used approaches for synthesizing Carbon dots (CDs) because it has numerous benefits over alternate approaches, such as being cost-effective, and environmentally friendly. Excellent photoluminescence and optical characteristics, higher yields, restricted size distribution, functionalization potential, enhanced stability and solubility, versatility, and compatibility with mass production are some of the benefits (Đorđević, Arcudi, Cacioppo, & Prato, 2022).

The process variables that determine CDs size, chemical composition, and crystallinity are the solvent, the reaction's temperature, reaction duration, and precursors' molecular structure. The specified reaction conditions are important because they have a significant impact on the precursor's reactivity and the segregation of the nucleation and growth phases of the resultant CDs (Khairol Anuar, Tan, Lim, So'aib, & Abu Bakar, 2021). Since the synthesis procedure requires carbonizing the carbon source, temperature is an important consideration in the development of CDs. The CDs typically consist of an amorphous carbon vicinity and a carbon graphitic core. Higher temperatures cause the core to grow while the amorphous region reduces simultaneously, influencing the optical properties. However, the reduction in quantum yield is typically caused by the carbonization of the surface groups. Therefore, the temperature range within which both the core as well as shell structures coexist is where the maximal quantum yield is attained (Jorns & Pappas, 2021). The degree of carbonization, quantum yield, photoluminescence (PL), and ultraviolet-visible (UV-vis) absorption spectrum are all clearly affected by reaction temperature, although functional groups, the amount of doping, and the lifespan of fluorescence of doped CDs are less affected (Zhang et al., 2016). The relationship between reaction temperature and reaction time in CDs' optical characteristics is significant. Similar to this, a longer reaction time leads to a larger degree of carbonization, which encourages the carbon core's formation and consequently, alters the associated CDs' optical characteristics (Papaioannou, Titirici, & Sapelkin, 2019). Since solvents can control precursor carbonization and dehydration, solvents are also a crucial parameter that governs the CDs' properties and characteristics. (Khairol Anuar et al., 2021). By altering the solvent concentration, the band gap associated with CDs can be readily optimized.

Furthermore, the precursors' carbon chains have an analogous effect on the fluorescence emission band.

1.2. Applications of Carbon Dots

By virtue of their physicochemical characteristics, applications for CDs are numerous and diverse. CDs have many key advantages, such as easy synthesis, inexpensiveness, high sustainability, colorful PL, non-toxicity, and exceptional biocompatibility. Such features have encouraged scientists to create novel materials with innovative uses and minimal ecological effect. As a result, CDs have versatile applications.

Whenever toxic chemicals such as pesticides, antibacterial agents, heavy metal ions, preservation agents, and nonbiodegradable compounds are present in food stuff over a specific permissible amount, it can lead to serious health problems. Given that heavy metal ions are capable of accumulating in vital organs and cause morbidities and complications, it is significant that these ions can be identified by utilizing CDs. These metal ions are detected by chemiluminescence (Gayen, Palchoudhury, & Chowdhury, 2019). The detection of multiple chemicals makes considerable use of CD-based logic gate sensors.

Strong adsorption properties, the ability to transfer and exchange electrons, and configurable emission are all characteristics of CDs. Their potential for usage in optoelectronic devices is therefore attractive. CDs are employed in electroluminescent devices as the active layer or as fluorescent downconverters (Y. Ding et al., 2017). CDs are great candidates for the role of sensitizer in solar cells due to their ability to acquire and transfer electrons easily (Mihalache et al., 2015). Similar to this, electron movement of a solar cell is accelerated with the addition of a CDs intermediary layer.

The electrocatalytic characteristics of CDs towards O_2 and H_2O_2 reduction are the primary focus of the few electrochemical biosensing applications that have been reported to date. These properties are utilized for the biosensing of glucose or H_2O_2 , as well as the sensing of dopamine, patulin, 2,4,6-trinitrotoluene, and glucose (Campuzano, Yáñez-Sedeño, & Pingarrón, 2019).

Due to their outstanding biocompatibility, water-soluble nature, nontoxicity, photoluminescence, and exceptional photostability, CDs are widely used in health and therapeutic chemistry for drug delivery, gene delivery, bioimaging, and the

development of effective biosensors (Gayen et al., 2019). CDs have tremendous potential as bioimaging agents. Fluorescence imaging has evolved into an efficient method to track biological activity within living cells because of its numerous characteristics, such as reduced radioactive risk, enhanced sensitivity, superior spatial resolution, and high-performance competence. A potential use of bioimaging is the gel electrophoresis method for detecting human serum proteins. (Na et al., 2013).

Due to their emissive properties, CDs served as a super drug carrier that made it possible to track drugs in both healthy and abnormal (disease-affected) cells. Due to their tiny size and high fluorescence, CDs are excellent candidates for drug delivery systems since they have significant cell membrane permeability. CDs may also turn magnetic once they are a component of a drug delivery system, making them crucial for MRI (Yao et al., 2017). MRI results become more accurate with CDs fluorescence. With CDs, numerous drugs can be delivered simultaneously.

However, the biocompatibility of CDs—that makes them potential candidates for usage in biomedical—is their most important biological characteristic. To quickly determine whether CDs significantly induce cytotoxicity in a human cell line, the MTT assay or the cytotoxicity assay can be utilized (S.-T. Yang et al., 2009). CDs currently serve as potential candidates for diagnostic applications.

Regarding the diagnosis and treatment of cancer, advancements in the domain of diagnostics are particularly ground-breaking. This is because lowering the risk of mortality from cancer requires early detection of the disease. Therefore, nanomaterials are incredibly essential to the field of oncological research in general if they may acquire the probability of cancer diagnosis at an early stage due to their enhanced capabilities at the nanoscale. Due to their unique physicochemical characteristics, CDs are an example of nanoparticles that are enabling important advancements in the field of cancer research (Li et al., 2019). The contributions in diagnosis are significant among the uses of CDs in relation to cancer. For the bioimaging of cancer cells, CDs can be coupled with particular compounds or functional groups. Some cancer cells overstate glutathione, a substance that eliminates free radicals. It has been suggested that CDs in conjunction with Fe^{+3} ions can be utilized to examine cancer cells with high glutathione expression (Gao, Jiang, Jia, Yang, & Wu, 2018). Additionally, CDs can be used to detect glycoprotein as a cancer biomarker. Different CDs surfaces have been

chemically functionalized to detect different glycoproteins that serve as cancer indicators. For instance, glycosylated nanocarriers made from CDs (Das & Mohapatra, 2017). Applications for cancer therapies include photothermal therapy, photodynamic therapy, and targeted drug delivery.

1.3. Introduction of Gold Nanoparticles

Gold's characteristics are highly distinct from those of its other group members and have FCC crystal structure. Michael Faraday pioneered the development of colloidal gold in the 1850s and gave it the term “Divided gold metal”, it's documented in his diary (Faraday, 1996). In earlier times, physicians and alchemists were aware of the special healing abilities of colloidal gold solution. One of the most ancient books explaining the therapeutic effects of derivatives of Gold was written in 1618 by philosopher and physician Francisco Antonii et al (Antonii). It features information on where to acquire colloidal gold, how to utilize it in medicine, and other useful recommendations. However, British researchers Faulk and Taylor pioneered the reference of AuNPs in modern medicine in 1971 (Faulk & Taylor, 1971). Researchers have utilized AuNPs for an array of biomedical and biotechnological applications because of their distinctive optical, physiochemical, and biocompatible features.

Gold nanospheres (AuNPs) are solid gold balls with a diameter that ranges from 5 to >100 nm produced by reducing chloroauric acid. The optical and electrochemical characteristics of AuNPs are greatly affected by the size, structure, interparticle separation, and surface chemistry. The distinctive optical characteristics of the gold nanoparticles are known as surface plasmon resonance (SPR).

Since the size of AuNPs determines the level of bioavailability, bioaccumulation, and cytotoxicity in a biological system, it plays a crucial role in the fabrication of efficient systems related to nanogold. Due to variations in its band gap coupled with size, gold's properties vary significantly in its nano form. As the particle or cluster size decreases, the spectral band gap of nanoparticles typically expands (Bansal, Kumar, Karimi, Singh, & Kumar, 2020). The physicochemical stability, further integration into cellular processes, and bioaccumulation of AuNPs are all facilitated by their surface charge, which is measured in terms of zeta potential. AuNP is less harmful than other NPs when utilized in a regulated way and doesn't interfere with the natural immune system of body by acting as an external substance (Y. Liu, Hardie, Zhang, & Rotello, 2017). The

toxicity level is significantly impacted by the particulate size, shape, surface charge, and concentration of AuNPs that has been assigned to them (Bansal et al., 2020). Lee et al. have also studied the cytotoxicity of AuNPs derived from green tea extract as a function of size and shape (Y. J. Lee, Ahn, & Park, 2019). The order of cytotoxicity was as follows: nanorods, nano stars, and nanospheres. According to this study, spherical nanoparticles are the most suitable for use in biomedical sciences.

The AuNPs have been studied in numerous clinical studies based on four crucial physical and chemical properties: chemical inertness, surface characteristics, electronic structure, and optical characteristics. The ability to produce AuNPs in multiple shapes due to their chemical inertness does not undermine their high stability, low toxicity, or immunogenicity, which are crucial properties for medicinal applications (Patil, Gambhir, Vibhute, & Tiwari, 2023). AuNPs also have a perk of being easily functionalized, which makes it easier to attach the appropriate compound to the surface. (Zhu et al., 2018).

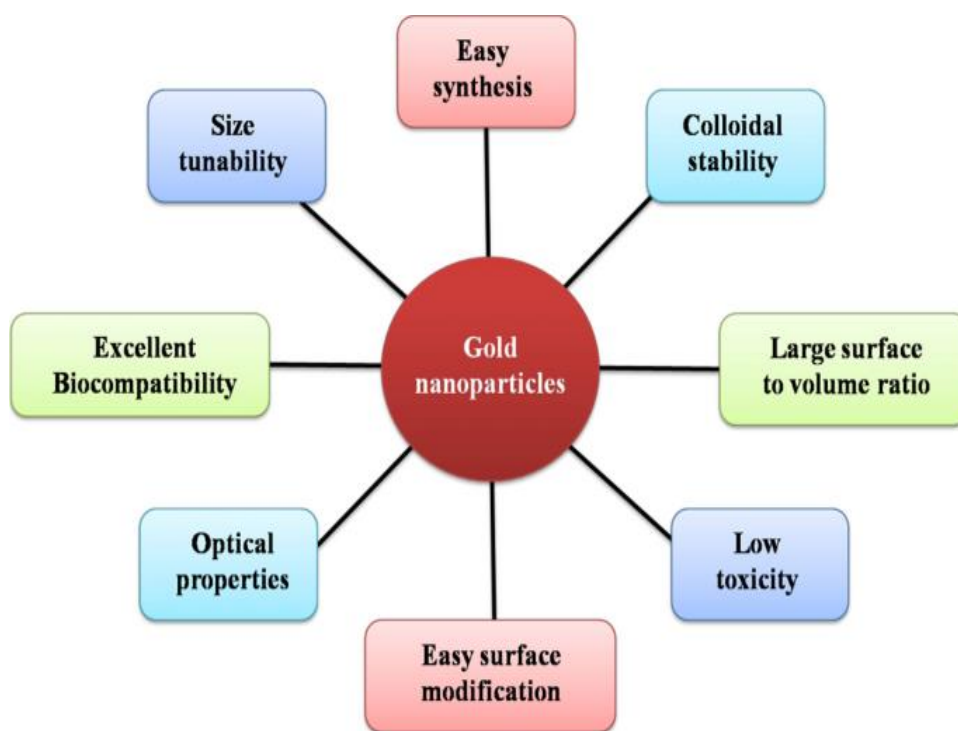


Figure 3: Gold Nanoparticles' Desirable Characteristics (Patil et al., 2023)

Evidently, the synthesis of AuNPs involves two stages: chemical reduction for the extraction of AuNP and stabilizations to stop further aggregation (Sani, Cao, & Cui, 2021). Precise and regulated synthesis is necessary due to the significance of AuNP

shapes and sizes in toxicological and biological applications. One of the most well-known, earliest, most simple, and reproducible methods to synthesize AuNPs was established by Turkevich in 1951 and depends on the reduction of HAuCl₄ through citrate in water (Turkevich, Stevenson, & Hillier, 1951).

In chemical reduction method, a reducing agent reduces gold ions, usually Au³⁺, to AuNPs. Common reducing agents include ascorbic acid, sodium borohydride, and sodium citrate. Electrons from the reducing agent move to the gold ions to drive the reduction process. To avoid the particles' aggregation, stabilizing chemicals of a certain sort are frequently added. (Zhao, Li, & Astruc, 2013). In photochemical synthesis, gold ions are reduced to nanoparticles by use of light, usually UV or visible light. In the presence of a photosensitizer, photons excite electrons, which causes gold ions to be reduced (Sani et al., 2021). At the electrode surface, gold ions are reduced during electrochemical synthesis. Gold ions undergo reduction to generate nanoparticles when a potential is applied at the working electrode (Zou et al., 2017). The sol-gel method entails making a sol that contains gold and then letting it go through a gelation process to create nanoparticles (Sonawane & Dongare, 2006). In biological synthesis, gold ions are reduced to nanoparticle size by means of biological organisms or their extracts. As reducing agents, various microbes, plants, and biomolecules notably proteins and enzymes can be used (Teimuri-Mofrad et al., 2017). The size, shape, stability, and scalability requirements of the outlined application should be carefully taken into account while selecting the gold nanoparticle synthesis process.

1.4. Applications of Gold Nanoparticles

Physicochemical properties of fine-scale AuNPs, such as quantified charging and discharge, non-toxic nature, biocompatibility, high surface-to-volume ratio, ease of surface modification, size tunability, photon-induced heating, electromagnetic radiation absorption and dispersion, optical and electronic properties, have made them highly desirable to scientists. Such characteristics have recently piqued the interest of biomedical researchers (X. Yang, Yang, Pang, Vara, & Xia, 2015).

Since ancient times, AuNPs have been employed for a variety of purposes, from tinting glasses to treating serious mental health issues. As a potent medication, colloidal gold has an extensive background of usage in therapeutic purposes. Palatable nano-gold has previously been used to treat psychological and rheumatic ailments in addition to dental

remediation. Additionally, it has been discovered that they boost immunity (Bansal et al., 2020).

With lab-on-a-chip, it is possible to detect and track pathogenic microbes (like viral and bacterial genomes), analyze nucleic acid immunological tests (antibodies to antigenic material, hormonal agents, etc.), track medical conditions (such as blood glucose or creatinine levels), analyze chemicals or proteins (such as cancer biomarkers in the bloodstream), perform DNA microarrays, and carry out other interventions. AuNPs have been used in numerous scientific initiatives, from the fabrication of lab-on-chips to biomedical applications (Anik, Mahmud, Masud, & Hasan, 2021).

AuNPs had earlier been utilized to study the development of antibodies and vaccinations towards over 45 pathogens that cause viral, bacterial, and parasitical ailments. For more than 20 years, AuNPs have been employed in biosensing and diagnostics. AuNPs can function as an electrochemical immunosensor at antibody-immobilized surfaces, boosting the electrochemical signal-transducing antigen-binding process. (Anik et al., 2021).

Conveniently conjugating AuNPs with radionuclides for diagnostic or medicinal objectives has prompted studies about nano-radiopharmaceuticals for imaging, therapy (primarily cancer therapy), biological distribution, pharmaceutical kinetics, and image-guided administration of cytotoxic anticancer drugs. AuNPs are gaining popularity among researchers for the transport of radioisotopes to cancerous cell and tissue populations because of their relatively low toxicology and elevated biotic half-life, even though the problem of biodegradability still exists (Silva, Cabral Campello, & Paulo, 2021).

Numerous studies using 3D cell culture tumors and animal models have demonstrated the effectiveness of AuNPs in combating cancer. Three categories of AuNPs-based cancer therapy exist: photothermal therapy (PTT), photodynamic therapy (PDT), and AuNPs-based anticancer drug delivery. The PTT process increases the temperature of the tumor microenvironment through the application of AuNP's light-to-heat conversion capabilities, which causes the tumor cells to undergo apoptosis or necrosis. PDT refers to a photochemistry-based therapy that works by combining molecular oxygen (O), photon energy (light), and a photosensitizer (PS) to cause cytotoxicity in

the tumor cell. The flexible interface chemistry between the Au and drug particles makes AuNPs-based anticancer drug delivery intriguing.

Although conjugated AuNPs, which have particle diameters that vary from 4 to 6 nm, are an excellent platform to disperse antibiotics and other antimicrobial peptides, bare AuNPs do not have any antibacterial effectiveness (Anik et al., 2021).

Similar to antibacterial agents, AuNPs can also be employed as antiviral agents. Functionalized AuNPs can be utilized solely or in conjunction with other compounds as an antiviral to obstruct virus entrance into a cell's host system (whether it's by simulating the virus-associated proteins and linking to the cell's receptors or through simulating the cell's receptor and linking to the virus-associated proteins), enhance drug delivery to the compromised cell, and prevent virus replication (Mehranfar & Izadyar, 2020).

AuNPs are among the numerous types of nanoparticles that are often employed as charge-trapping materials in non-volatile storage systems because of their significant work function, ease of synthesis, and chemically stable nature. Excellent stability as memory devices can be found in AuNPs coated with an adequate insulator, and this insulation helps prevent the accumulation of charges after the applied field is removed (J.-S. Lee, 2010).

AuNPs' unique optical characteristics and high surface-to-volume ratio enable highly selective and sensitive detection. The health and wellbeing of humans is adversely affected by heavy metal ions, which are typically toxic. They are classified as environmental contaminants and have the potential to cause serious harm to human health. The plasmon absorption peak shifts and color alters when AuNPs aggregate due to interaction with particular metal ions. This characteristic of AuNPs has been used to detect heavy metal ions in aqueous solutions calorimetrically (Priyadarshini & Pradhan, 2017).

In neutral and alkaline solutions, AuNPs have an intriguing activity for glucose oxidation. Due to its capacity to overcome the instability of glucose oxidase, which is a shortcoming of standard glucose biosensors, The enzyme-free electrochemical glucose biosensors with AuNP-modified surfaces have drawn significant attention. The

diagnosis and treatment of diabetes may undergo significant changes as a result (Chang et al., 2014).

1.5. Gold Coated Carbon Dots (AuCDs)

Water solubility doesn't affect the chemical inertness of CDs. Furthermore, their functionalization is incredibly simple. They are particularly attractive for plenty of applications in bioimaging, photocatalysis, nanomedicine, and other areas because of their exceptional characteristics, notably great photobleaching resistance, low toxicology, exceptional biocompatibility, and electron acceptor/electron donor ability. As active components for electrochemical (bio)sensors, CDs are also ideal. Integrating them to other nanoparticles (NPs) can increase their electrochemical activity even more. Gold nanoparticles (AuNPs) are among numerous metal NPs that are biocompatible, non-toxic, and relatively simple to disperse. These and other distinctive characteristics made them well-liked catalysts for uses in the biomedical, biotechnological, and sensory disciplines.

The biocompatible nature of AuNPs persists to open up a multitude of avenues in the domain of theranostics. Metal nanoparticles have become prevalent in biomedical science because of the easy functionalization of their surfaces. Modern medical research requires the use of biocompatible, water-soluble gold nanoparticles that can abide in physiological media. For the organic shell to exhibit water solubility characteristics, hydrophilic termini must be functionalized (Hameed et al., 2018).

CDs are characterized by strong fluorescence, exceptional dispersibility, and excellent biocompatibility. The output of photoacoustic signals, stability, and photothermal conversion efficiency tended to be superior in AuCDs. AuCDs are suitable for biomedical applications because of their low toxicity. In analogy to bare Carbon dots, the AuCDs showed higher fluorescence intensity and greater photostability. The higher fluorescence competency made it possible to image biological specimens with greater sensitivity and accuracy.

1.6. Aims and Scope

This research concentrates on the synthesis and comparison of physiochemical and biocompatibility evaluation of Carbon Dots (CDs) and Au-coated Carbon dots (AuCDs).

1.7. Objectives of the Study

Specific objectives of the research incorporate:

- ❖ Chemical synthesis of CDs from ascorbic acid using the hydrothermal method
- ❖ Confirmation of fluorescence property of newly synthesized CDs
- ❖ Characterization of CDs using UV-Visible spectroscopy, SEM, XRD and FTIR
- ❖ Synthesis of AuCDs
- ❖ Characterization of AuCDs using UV-Visible spectroscopy, SEM, XRD and FTIR
- ❖ Optical Detection of Metal ions using CDs and AuCDs
- ❖ Electrochemical Biosensing of Glucose via CDs and AuCDs
- ❖ Cytotoxicity assay on HEK and MDA-MB-231 of CDs and AuCDs

Chapter 2

LITERATURE REVIEW

2.1. Optical Detection of Metal Ions

CDs serve as tools for selective and sensitive fluorometric and colorimetric metal ions detection because their surface oxygen moieties integrate with metal ions to cause the PL to quench. The energy transfer among nanocarbons and metal ions through selective interactions caused by surface traps and functional groups is the primary cause of PL quenching. Selectivity is affected by all the properties of nanocarbons, notably size, shape, edge structure, and surface functionalities.

Abhay Sachdev et al. (Sachdev & Gopinath, 2015) synthesized fluorescent CDs using coriander leaves via hydrothermal synthesis, negating the necessity for supplementary passivating reagents for modification of the surface. Their study demonstrated the pH-regulated optical sensitivity of the proposed CDs to Fe (III) detection. Low quenching efficacy was found under acidic ($\text{pH} < 7$) & more basic ($\text{pH} > 9$) conditions attributed to the protonation of surface carboxylic groups. The CD-Fe (III) complex's interactions weakened as a result, and Fe (III) complexed with hydroxyl groups rather than CDs. The deprotonation of surface carboxylic groups was observed to be responsible for the enhanced Fe (III)-CDs interaction observed within the pH range of 7 to 9.

As it boosts the immune system and strengthens bones, the optimal growth and development of biological activities requires copper (Cu^{2+}). However, excessive Cu^{2+} can lead to pain, vomiting, and disruptions in biological activity. Zheng et al. (Zheng, Liu, Gai, Tian, & Ren, 2019) synthesized CDs using an eco-friendly, straightforward pyrolysis process that excluded complex post-processing treatment. The CDs showed a 25% quantum yield and a prominent fluorescent peak at 468 nm. As a result of the complexation between the amino acid groups embellished on the CDs surface and the adsorbed copper ions, the CDs demonstrated a potent fluorescence response to $70 \mu\text{M}$ Cu^{2+} , alongside a sensitivity of approximately 77%. They also demonstrated excellent stability, exceptional selectivity, and quick response times—less than a minute.

Applications such as disease diagnostics, forensics, food, and environmental monitoring require precise and efficient detection of biological and chemical entities. AuNP-based colorimetric assays have been utilized for detecting a range of analytes, that include proteins, nucleic acids, metal ions, and small molecules. AuNPs have been a top choice for colorimetric applications over other metals and polymer nanoparticles because of their superior surface plasmon resonance (SPR), that leads to a characteristic color formation.

Since heavy metal ions readily complex with AuNPs and are widely found in pollutants, they are the most studied analytes among other metals. Given that AuNPs and metal ions chelate quickly, aggregation-based detection sensors are frequently constructed. Compared to electrochemical sensors, AuNPs-colorimetric sensors have not been studied as much in the field of inorganic ion detection. While biosensors are commonly used to detect bio-analytes, chemo-sensors are extensively employed to detect organic analytes. Colorimetric sensors based on AuNPs have the potential to address future concerns related to food safety, wastewater treatment, and pollution removal (Sadiq, Safiabadi Tali, Hajimiri, Al-Kassawneh, & Jahanshahi-Anbuhi).

2.2. Electrochemical Biosensing of Glucose

The primary energy source for cellular functionality in the living body is glucose. Retaining an optimal concentration of glucose in the blood is essential. Researchers have concentrated on carbon-based nanomaterials because of their distinctive characteristics, such as excellent stability, substantial definite surface area, chemically inert nature, and superior conductivity. The carbon-based nanomaterials can be utilized as electrodes or facilitating matrices in the electrochemical sensing process to achieve numerous objectives, notably enhancing the electrocatalytic performance, enhancing electron transit across the interface, and ensuring enhanced biocompatibility for signal amplification (Cho, Kim, & Park, 2020).

Hanxu Ji et al. (Ji et al., 2016) used polyacrylamide to synthesize nitrogen-doped CDs in a single step. The excellent stability, sensitiveness, and accuracy of the biosensor in determining glucose are due to Nitrogen-induced charge decentralization at N-doped CDs, enhancing the electrocatalytic efficiency for the reduction of O₂, and the strong adherence in GO_x by amino-carboxyl chemical reactions for the enzyme's immobilization. The designed biosensor has a 0.25mM detection limit and responds

adequately to glucose over a concentration range of 1 to 12mM in serum samples. With excellent stability and reproducibility, the novel biosensor can detect glucose with high selectivity under physiological conditions.

AuNPs are used frequently to fabricate electrochemical biosensors with upgraded analytical performance compared to other biosensor designs because of their distinctive capabilities to provide an appropriate microenvironment for biomolecules immobilization while sustaining their biological activity, and To stimulate the transfer of electrons between the electrode surfaces and the biomolecule's redox site (Pingarrón, Yáñez-Sedeño, & González-Cortés, 2008).

A literature review suggests that integrating AuNP with a carbon-based nanomaterial, the modified electrode's sensitivity can be significantly enhanced, boosting the electrochemical biosensor's analytical efficiency. (Alim, Vejayan, Yusoff, Kafi, & Bioelectronics, 2018). High electrocatalytic activity towards glucose is demonstrated by the CQD/AuNP-GO_x biosensor. Given the excellent sensitivity, substantial reproducibility, and selectivity attained at such a nano-hybrid-based biosensor, this is anticipated to be an incredibly potential matrix for use in the immobilization of other biorecognition components. Furthermore, despite the presence of potential interfering agents, the fabricated biosensor displays acceptable relative error findings when used to measure the glucose concentrations in human serum specimens (Buk, Pemble, & Twomey, 2019).

Using AuNP-CN nanocomposites has numerous advantages, notably feasible surface modification, excellent electrical conductivity, superior sensitivity, and selectivity due to their the capability to identify an analyte's oxidation potential (Cho et al., 2020). Based on the AuNP/CQDIL composites, the electrochemical (bio)sensors for BPA demonstrated excellent analytical efficiency, such as lower detection limit, strong sensitivity, broad linear span, superior selectivity, and sufficient reproducibility (Örenli, Kaçar Selvi, Öztürk, Erden, & Kılıç, 2023).

2.3. Cytotoxicity Assessment

Since a major cause of mortality in humans is cancer, it has been extensively studied in the past in both the medical and scientific domains. Hence, early detection of cancer markers increases the likelihood that treatment will be successful and improves the

quality of life for cancer patients, which is why early cancer diagnosis is essential to lower the percentage of cancer-related deaths.

V.P. Sangeetha et al. (Sangeetha, Smriti, Solanki, & Mohanan, 2021) synthesized high quantum yield Zwitterionic Carbon dots. Its safety evaluation on HEK-293 cells was done at distinct concentration ranges ($50\text{--}1600\ \mu\text{g mL}^{-1}$). Zwitterionic CDs cause nuclear condensation, ROS induction, and mitochondrial dysfunction at higher concentrations. Furthermore, apoptosis is induced at higher concentrations by pro- and anti-apoptotic gene mRNA expression profiles of zwitterionic CDs through an intrinsic mitochondria-mediated pathway. According to this study, $50\text{--}200\ \mu\text{g/mL}$ is the secure range for the intended use.

It has been shown that target-specific administration of Co^{2+} doped biotin-functionalized fluorescent Carbon dots (CoCD_b) can differentiate cancerous cells from non-cancerous ones and cause cancer cells to die selectively by causing hypoxia-induced apoptosis due to stabilized HIF-1 α . The HIF-1 α protein functions as a pro-drug since Co^{2+} of CoCD_b is present. Prodrug activator Co^{2+} inhibited PHD activity, causing cancer cells to undergo apoptosis, which changed the expression of prodrug HIF-1 α protein. Compared to non-cancer cells (NIH3T3 and HEK-293), CoCD_b demonstrated approximately a 3-3.1-fold increase in the death of cancerous cells (MDA-MB-231 and HeLa). Using an immunoblotting assay on MDA-MB-231 cells treated with CoCD_b , it was determined that the efficient killing of cancerous cells was caused by increased expression of HIF-1 α . CoCD_b -treated cancer cells demonstrated notable apoptosis in 2D cells and 3D tumor spheroid, suggesting that CoCD_b can serve as an efficient theranostic agent (Chowdhury, Pal, Ghosh, & Kumar Das, 2023).

Using fluorescence-based assessments in cultured cells, Jeyarani et al. (Jeyarani et al., 2020) synthesized biomimetic Au nanoparticles using the marine seaweed *Gelidium pusillum* (*G. pusillum*) to assess their cytotoxic and biocompatible properties. The seaweed extract plays an integral part in stabilization of the AuNPs to prevent their aggregation and coalescence. At an IC_{50} of $43.09 \pm 1.6\ \mu\text{g mL}^{-1}$, the biomimetic AuNPs were observed to be cytotoxic to cancerous cells (MDA-MB-231). Contrarily, biomimetic gold nanoparticles demonstrate noteworthy biocompatibility against human embryonic kidney cells, even at a concentration of $150\ \mu\text{g mL}^{-1}$. Fluorescence assays

based on morphological analysis verified that biomimetic gold nanoparticles can induce apoptosis, which in turn kills cancer cells.

Using natural phytochemicals (Curcumin: Cur, Turmeric: Tur, Quercetin: Qu, and Paclitaxel: Pacli), SK Vemuri et al. (Vemuri et al., 2019) synthesized and evaluated multiple biosynthesized AuNPs (b-AuNPs). The b-AuNPs' anti-cancer potential was assessed in multiple breast cancer cell lines, such as MCF-7 and MDA-MB-231. Comparing the combinations of AuNPs-Cur, AuNPs-Tur, AuNPs-Qu, and AuNPs-Pacli with individual treatment the aforementioned phytochemicals or the nanoparticles revealed that Breast cancer cell apoptosis, replication, angiogenesis, colony genesis, and formation of spheroid were all suppressed most therapeutically by the combinations, indicating a synergistic effect. The human embryonic normal kidney cell line (HEK-293) did not exhibit any cytotoxicity when exposed to either of the nanoconjugates alone or in combination, indicating their biocompatibility. The study that demonstrated the prospective anti-cancer capabilities of b-AuNPs using a multifaceted approach suggests that such nanoparticles may represent a new era of cancer nanomedicine owing to their low toxicology and great therapeutic efficacy.

Chapter 3

METHODOLOGY AND CHARACTERIZATION TECHNIQUES

This research study focused on the synthesis, characterization, surface functionalization and applications of Carbon Dots. Additionally, Gold-coated Carbon Dots were synthesized to achieve optimal physiochemical properties for its further use in Biomedical applications. The materials and methods used to conduct this research are as follows:

3.1. Chemical Reagents

The chemical reagents employed in the research are as follows:

Chemicals	Molecular Formula	Molar Mass (g/mol)
L-Ascorbic Acid	$C_6H_8O_6$	176.12
Ethylenediaminetetraacetic acid Disodium salt Dihydrate (EDTA)	$C_{10}H_{14}N_2Na_2O_8 \cdot 2H_2O$	372.24
Hydrogen Tetrachloroaurate(III) Trihydrate	$HAuCl_4 \cdot 3H_2O$	367.79
Sodium Citrate	$HOC(COONa)(CH_2COONa)_2$	294.10

3.2. Synthesis of Carbon Dots

The process of hydrothermal carbonization of ascorbic acid was used to yield CDs. The yield of highly fluorescent CDs produced by this process has been documented in the literature (Ortega-Liebana, Encabo-Berzosa, Ruedas-Rama, & Hueso, 2017). Their procedure was modified slightly by adding EDTA, prolonging the reaction time, and altering the purification steps.

3.2.1. Hydrothermal Carbonization

The hydrothermal carbonization process was conducted in a Teflon-lined stainless-steel autoclave (TI0100). The hydrothermal reactor in use here is a metal autoclave with a Teflon lining. It may also sometimes contain a gold, platinum, or silver tube to protect the autoclave's body from any corrosive substances that may be present in the reactant mixture within.

3.2.2. Synthesis Reaction

Since Ascorbic Acid (AA) was the carbon source in this process, 1M solution was prepared by adding 17.61g of L-Ascorbic Acid (Sigma Aldrich, Germany) in 100 ml of DI water. The mixture was placed on the magnetic stirrer for 5-10 minutes so that it could be properly dissolved. Then EDTA was added 1% by weight to the solution and was further stirred for 5-10 minutes. The resulting solution was poured in the Teflon lined autoclave which was sealed fully to avoid leakage. Then for 24 hours, this autoclave was kept in an oven incubator at 200°C. Once this reaction was completed, the autoclave was cooled back to room temperature and the solution inside was subsequently retrieved. This solution was supposed to be yellowish brown in color with a burnt scent. The solution was centrifuged at 6000 rpm for 30 minutes and the agglomerates formed during the carbonization process were therefore removed. Further purification of the supernatant from this centrifugation was carried out using a 0.22µm syringe filter. This filter removed large particles which were unable to pass through the filter. The solution obtained after this step was dark yellow/light brown in color. This solution contained AA CDs.

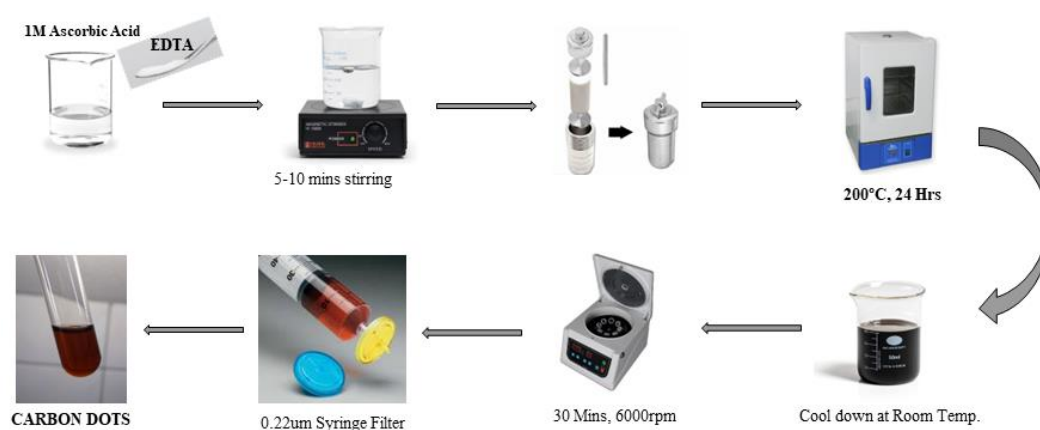


Figure 4: Synthesis, Assembly and Storage Process of Carbon Dots

3.3. Synthesis of Au-Coated Carbon Dots (AuCDs)

A simple coating procedure was used to synthesize Au-coated CDs (Lo, Xiao, & Choi, 2007). 0.1mM solution of Au precursor was prepared using $\text{HAuCl}_4 \cdot 3\text{H}_2\text{O}$ salt and DI water. An aqueous solution of HAuCl_4 (0.01mM) was heated and stirred to boiling. Then, 0.03mg/ml of as-prepared CDs solution and sodium citrate (1% by weight) were added to the reaction mixture while being stirred. The solution turned purple gradually, initially colorless. The reaction mixture was further boiled along with stirring for 10 minutes. The obtained purple solution is AuCDs.

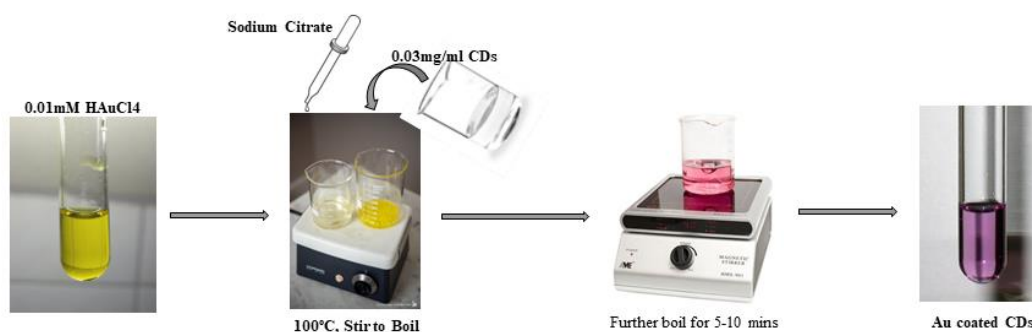


Figure 5: Synthesis, Assembly and Storage Process of Carbon Dots

3.4. Characterization of CDs and AuCDs

The process of fabricating and synthesizing the requisite materials allows to evaluate them both qualitatively and quantitatively, which helps to justify the claim that the material has been obtained in its best configuration. The study directs towards multiple characterization methods that employ electrochemical and distinct spectroscopies to examine the substance. These techniques, along with information about morphology, structural characteristics, electrochemical properties, and optical characteristics, facilitate the identification of successful synthesis.

Following is a list of some of the notable characterization techniques that have been utilised. The fundamental working principle of it is then explained in detail separately.

- ❖ X-Ray Diffraction (XRD)
- ❖ Ultraviolet Visible Spectroscopy (UV-Vis)
- ❖ Fourier Transform Infrared Spectroscopy (FTIR)
- ❖ Scanning Electron Microscopy (SEM)

- ❖ Energy Dispersive X-Ray Spectroscopy (EDX)
- ❖ Electrochemical Workstation
- ❖ Cytotoxicity Assessment

3.4.1. X-Ray Diffraction (XRD)

For elemental analysis and phase identification, non-destructive techniques as X-ray diffraction (XRD) are employed. The technique is effective for determination of the crystallite size, domain and grain size, crystal orientation, crystal structure, and interlayer spacing. Utilizing Bragg's law of diffraction, the method is principally employed for phase identification.

Components of X-ray Diffractometer

The three primary components of an X-ray diffractometer are as follows:

1. Cathode ray tube or X-ray tube
2. Sample holder
3. X-ray detector

Electron production occurs within the cathode ray tube due to a heated filament. As a result of the supplied potential, the electrons accelerate towards the target material. Upon impact, the target material's inner shell electrons are displaced by these highly energized electrons, resulting in the production of X-rays. The sample is exposed to these X-rays, which are partially reflected. X-rays can experience diffraction and interference phenomena because they are electromagnetic radiation. Following the diffracted beams being detected by the X-ray detector, a graph is plotted between the intensity of the diffracted beams and 2θ , the angle between the incident and reflected beams.

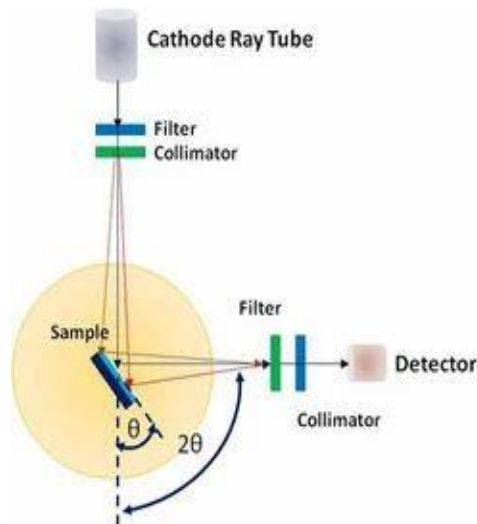


Figure 6: X-ray Diffractometer (Despotopoulou, 2019)

Fundamental Principle of X-ray Diffraction

A collection of atoms organized on lattice planes constitutes crystals. A distance 'd' separates each plane from the one adjacent to it. W.L. Bragg's explanation states that incident rays of electromagnetic waves, or X-rays, are partially reflected from adjacent planes when they strike crystals (Figure 7). Constructive interference from these reflected rays is dependent upon the fulfilment of Bragg's criterion i.e.,

$$2d\sin\theta = n\lambda$$

where, n = positive integer

λ = wavelength

d = interplanar spacing

θ = angle between incidents and reflected X-rays.

It's known as Bragg's law. Diffracted beams are characterized as reflected rays that constructively interfere. They contain information about the crystal structure of materials and are detected by the XRD detector.

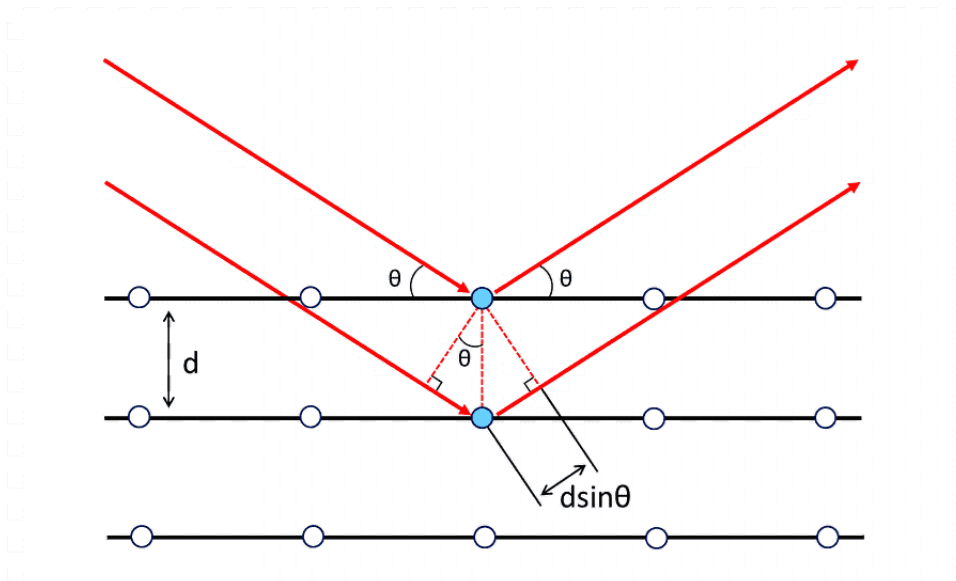


Figure 7: Bragg's Law Schematic (Venkata Sivareddy, Krishna, & Venu Gopal, 2022)

Peak position, width, and geometry of the diffraction pattern, which originate from the detector, are used to analyze the material, and provide information about its composition. The plane's presence in the crystal structure can be determined from the angle at which the peak lies.

3.4.2. Ultraviolet Visible (UV-Vis) Spectroscopy

Using a reference or blank sample as a comparison, UV-Visible spectroscopy is an analytical technique that determines the distinctive wavelengths of UV or visible light that the specimen absorbs or transmits. The characteristic is influenced by the sample's composition and may provide insight into the concentrations and composition of the sample.

Fundamental Principle of UV-Vis Spectrophotometer

The basic principle of Ultraviolet-visible (UV-visible) spectroscopy is that distinct chemical compounds absorb different wavelengths of light, generating distinctive spectra. The correlation between matter and light is the basis of spectroscopy. A spectrum emerges as a result of the excitation and de-excitation that occurs when matter absorbs light.

UV spectroscopy is based on the Lambert-Beer Law. According to Beer and Lambert's laws, the path length (ℓ) and solution concentration (c) are directly proportional to the absorbance (A) of an incident monochromatic beam. The rate at which monochromatic

light intensity decreases is directly proportional to the medium's thickness (m) and the dilution's absorbing substance's concentration (c). Mathematically,

$$A = \epsilon * l * c$$

where c is the concentration of the absorbent species,

l is the sample cell's path length,

ϵ (epsilon) is the molar extinction or absorptivity coefficient,

A represents absorbance.

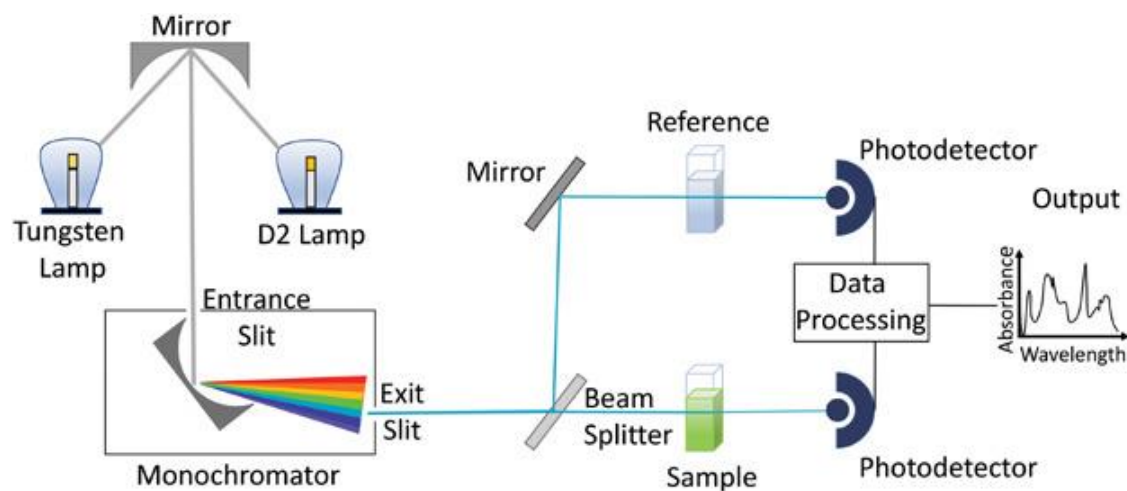


Figure 8: UV-Visible Spectrophotometer (Rocha, Gomes, Lunardi, Kaliaguine, & Patience, 2018)

3.4.3. Scanning Electron Microscopy (SEM)

The multifunctional scanning electron microscope generates a precisely detailed image of the specimen's surface by using a concentrated electron beam. The sample's chemical composition and surface topography are demonstrated through the electron beam's interaction with the material.

Components of SEM

A scanning electron microscope is made up of many components. Some essential components are:

1. A high-energy electron gun that both creates and accelerates electrons.
2. Electromagnetic apertures and lenses concentrate and outline the electron beam.

3. Scanning coils as deflectors. The scanning coil's main function is to concentrate and then redirect the electron beam.
4. Sample chamber for accumulating, repositioning, and modifying samples at different angles.
5. Electron detectors that are secondary and backscattered. Transforming an electrical current into a visual and projecting it onto the screen is the detector's main function.
6. Vacuum chamber to prevent any deviations that could disperse electrons. To generate the vacuum, a vacuum pump is utilized.

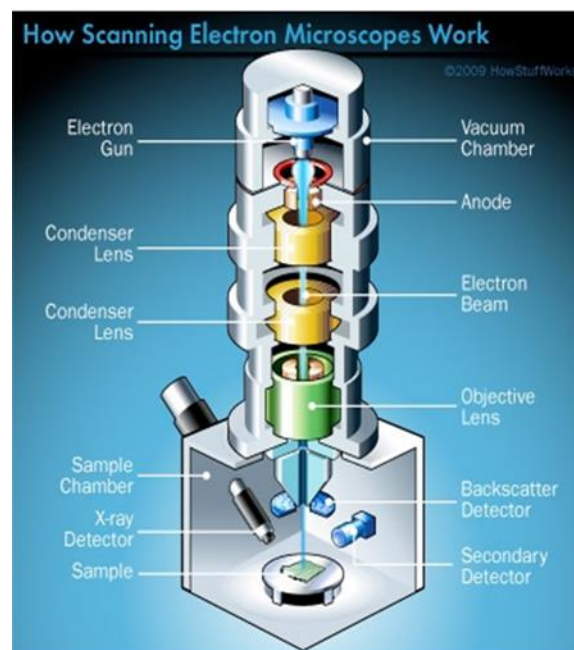


Figure 9: Schematic Diagram of SEM (Ananthapadmanaban, 2018)

Fundamental Principle of SEM

Multiple phenomena occur as the sample and electron beam interact;

Emission of Secondary Electrons: The sample's surface layer atoms' outer shell electrons interact with the electron beam, leading to the production of secondary electrons, also known as auger electrons.

Backscattered Electrons: Electrons retreat elastically from the sample; means they don't transfer their energy to other electrons.

Radiation Emission: As the core-shell electrons of the specimen atoms interact with an electron beam, Characteristic X-rays are generated.

The backscattered electron detector and secondary electron detector identify the backscattered electrons and secondary electrons. These electrons are accountable for analyzing the sample's morphology.

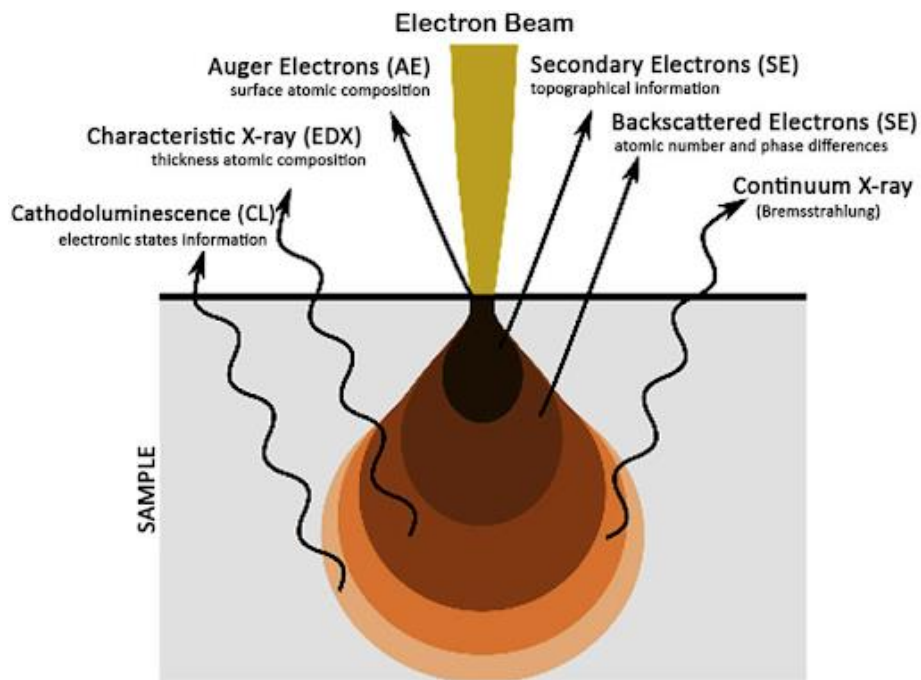


Figure 10: Working Principal of SEM (Ezzahmouly et al., 2019)

3.4.4. Energy Dispersive X-Ray Spectroscopy (EDX)

Although it can also be used for semi-quantitative analysis, Energy Dispersive Spectroscopy, also referred as Energy-Dispersive X-ray Spectroscopy, is usually employed in qualitative material analysis.

In addition to X-rays, which are used for element identification and quantification, the SEM/EDX system generates a wide range of signals, such as secondary and backscattered electrons, which are employed for morphological analysis and image generation. The EDX detection limit is influenced by the sample's surface condition; smoother surfaces typically have a lower detection limit. With EDX, elements with major (>10wt%) and minor (about 1–10wt%) concentrations can be determined. It is also possible to identify bulk materials (0.1 wt%) and trace elements (< 0.01 wt%) (Kothleitner et al., 2014).

The following are a few of the main advantages of EDX:

1. An efficient elemental analysis method; generally. With the exception of light elements like boron, it can detect almost every element.
2. Raster scanning: Scan particular, single-spot regions. Its wide range extends from approximately 1 mm² to submicron.
3. The electron microscope's image can be connected to the elemental spectrum.
4. The obtained data can be used to create "dot maps," also known as "elemental maps."
5. A technique that is nondestructive because it only penetrates the specimen's surface by a few microns.

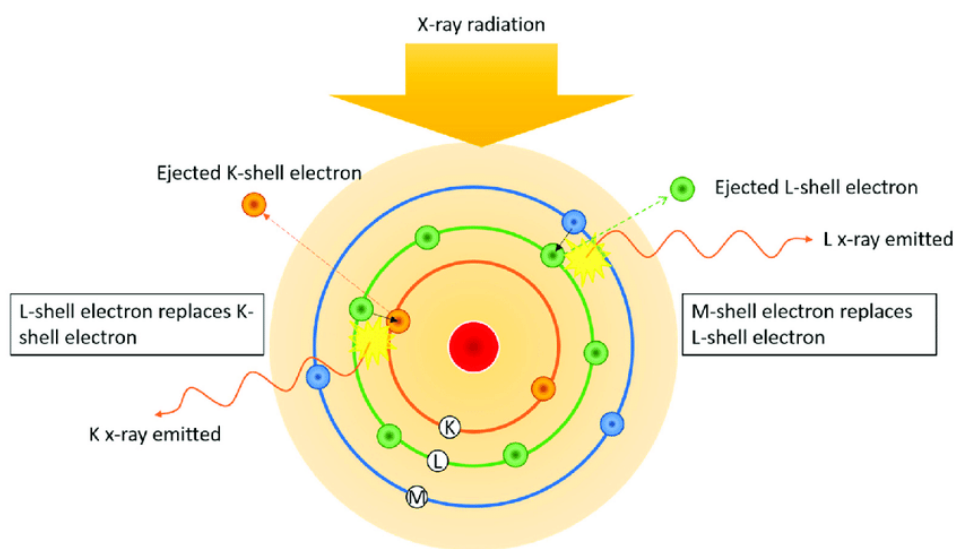


Figure 11: Working Principal of EDX (Long, Nand, & Ray, 2021)

3.4.5. Fourier Transform Infrared Spectroscopy (FTIR)

FTIR spectroscopy can be utilized to determine functional groups in a material. Every material has a distinct fingerprint region, which ranges from 1 to 1500 cm⁻¹, on the FTIR graph. By comparing the FTIR graph's peaks to the reference ones, thereby aids in sample identification.

Working Principal of FTIR

Infrared light is produced by an I.R. source and passes through the interferometer. The interferometer uses a beam splitter to split the light into two directions that are perpendicular to each other. There are two mirrors in the interferometer as well; one is stationary, while the other is movable. Two split perpendicular beams are directed towards the stationary mirror and the moveable mirror, respectively. The two beams

then return to the beam splitter and recombine. Constructive and destructive interference are caused by the moveable mirror, which changes the path length between the two beams. Next, as the recombined beam falls upon the sample, it interacts with it. As they contact, specific wavelengths of light are absorbed while the remainder of the light is transmitted. The detector, that captures the information about light absorption at each wavelength, detects the transmitted light. This is subsequently translated to the inverse domain, or wave number, via the Fourier transform, yielding the desired transmittance vs. wave number graph.

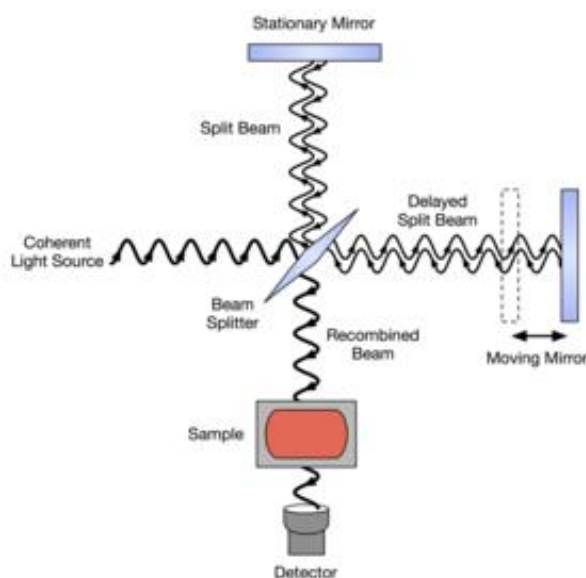


Figure 12: Schematic Working of FTIR (S. K. Rahi, Hassan, & Abd, 2016)

3.4.6. Potentiostat

In electrochemical research, potentiostat, also known as electrochemical workstations, are essential measurement and regulation systems that are used to evaluate the oxidation and reduction mechanisms connected to chemical reactions in active materials.

The working electrode and reference electrode's voltage differential is controlled, and the current flowing between the working electrode and counter electrode is then measured.

Configuration of Potentiostat

The working, counter, and reference electrodes of a conventional three-electrode cell are all immersed in the same electrolyte. In the process of three electrode investigations, the working electrode's potential is measured with respect to the reference electrode, and charge flow (current) mostly happens between the working and the counter electrode. Usually, a potentiostat has six leads, each with a distinct color clip.

The following is the objective of each electrode:

1. The electrochemical reaction is carried out by the **Working electrode**. It receives voltage applied to it in relation to the potential of the reference electrode. An "inert" substance, such as glassy carbon, platinum, or gold, serves as the working electrode. In these situations, the electrochemical reaction occurs on a surface that is provided by the working electrode.
2. A known and stable equilibrium potential is possessed by the **Reference electrode**. Against the other electrodes in the electrochemical cell, it serves as a reference point. A reference electrode is used to determine the applied potential (V). This electrode maintains nearly zero current flow. Ag/AgCl and Hg/HgO electrodes are the most often utilized reference electrodes.
3. The **Counter electrode** completes the cell's electrical circuit. As electrons go from the counter electrode to the working electrode, the current is measured.

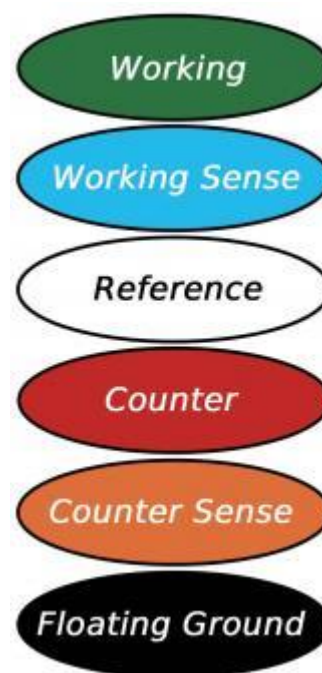


Figure 13: Color Scheme of 3-electrode setup

3.4.6.1. Cyclic Voltammetry (CV)

Cyclic voltammetry (CV) is a robust and well-known electrochemical technique to evaluate the reduction and oxidation processes of molecular entities. Additionally, electron transport-mediated chemical processes like catalysis require the use of CV. CV is a beneficial technique for determining the mechanism of the electron transmission reaction taking place in the material.

Using the method known as Cyclic voltammetry (CV), an electrode is submerged in a solution with a known molarity. The current flow is then determined by adjusting the potential of one electrode and calculating the voltage required for transferring an electron between the electrodes and the target molecule. A potentiostat, which is attached to these two electrodes, regulates the voltage that flows between them. It is governed by Ohm's law.

In CV, the control voltage is swept linearly between two voltage values. Information regarding the electrochemical reactions taking place at the working electrode is contained in the current generated by the cyclic voltammograms, which is dependent upon the applied voltage and scan rate. There may be two peaks on the CV curve: one for oxidation and one for reduction. The amount of kinetics at the electrode surface determines how many peaks appear on the curve. The redox species upon the electrode's surface are governed by the applied potential.

The cyclic voltammeter's peak potential (E_a and E_c) and peak current (I_p and I_c) are essential parameters.

Fabrication of Working Electrode

Glassy carbon electrode (GCE) was used to fabricate the working electrode. Prior to the fabrication of the working electrode, GCE was polished using a 0.05 mm alumina slurry after being thoroughly rinsed with DI water (Beuhler). The electrode was then ultrasonic cleaned with ethanol and water, and then dried. NPs were deposited on the GCE by drop cast method and air dried to make a thin film.

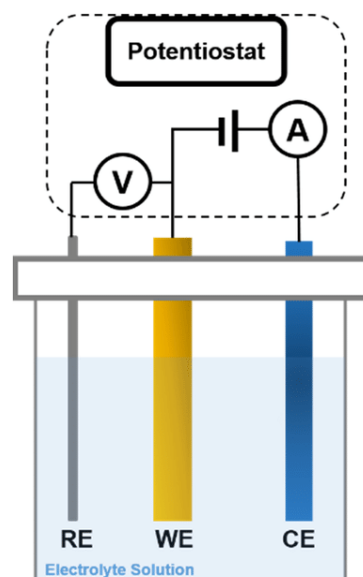


Figure 14: Schematic of an electrochemical cell

3.4.7. Cytotoxicity Assessment

A chemotherapeutic agent's ability to cause toxicity to living cells is known as Cytotoxicity. In order to determine the intended biomedical usage of nanoparticles, cytotoxicity assessments are crucial.

The ability of CDs and AuCDs to be toxic towards cancer cells was tested by checking the percentage cell viability of HEK-293T and MDA-MB-231 cells through MTT assay with CDs and AuCDs.

Culturing of Cell Lines

For the cytotoxicity assay, two cell lines have been cultured using RPMI-1640 culture media that had been modified with 10% heat-inactivated fetal bovine serum (FBS) (Sigma Aldrich, USA) and 2% Penicillin-streptomycin antibiotic.

❖ HEK-293T

It is an immortalized-positive human embryonic kidney cell line.

❖ MDA-MB-231 (M.D, Anderson – Metastatic Breast 231) (ATCC® HTB-26TM)

It is a triple-negative breast cancer cell line (TNBC).

Subculturing of Cell Lines

HEK-293T and MDA-MB-231 cells were allowed to grow in a T25 cell culture flask of 25 cm² and their confluency was measured under the inverted microscope. As the confluency reached 60-70%, Through pipetting, the cells' existing media was eliminated and the cells were subsequently rinsed with 2 ml of autoclaved, 0.01M phosphate-buffered saline (PBS) for cell culture (Sigma Aldrich, USA). After that PBS was removed and 2ml of trypsin-ethylenediaminetetraacetic acid (EDTA) (Sigma Aldrich, USA) was added and incubated for 2 mins at 37°C to de-adhere the cells. Both the adherent cell lines were gently tapped to scrap the cells of the flask's surface and were visualized under the microscope to confirm the detachment of cells that were seen floating. The cells were collected and transferred to a falcon tube and centrifuged at 2000 RPM for 2 mins to obtain the cells in the pellet. The supernatant was discarded, and the obtained pellet was resuspended in the RPMI complete media. The mono cell distribution of the cells was ensured by mixing the cells through

pipetting. The obtained cells were implanted in a 25 cm² flask at 1 × 10⁵ cells/ml density and were incubated under optimum conditions of 5% CO₂ and 37°C temperature.

NPs Dilutions and Plating

96-well plates were needed for MTT Assay. One plate was required for cytotoxicity evaluation of each cell line because there were 7 dilutions of CDs and AuCDs, one positive control and one negative control. The number of cells per well was kept at 10,000 and the calculation of number of cells was used to assess how much volume of the media containing cells was to be added to each well. All these dilutions were to be added to the 96-well plate with a volume of 200 µl in each well. Once these dilutions had been added to the plate, it was then covered and wrapped with aluminum foil without disturbing the cells. These plates, now prepared, were put in the incubator with temperature at 37°C and CO₂ at 5%.

MTT Assay

The cytotoxicity of CDs and AuCDs was measured through the MTT assay, which is a measure of cellular metabolic activity which indirectly gives insights into cytotoxicity, viability and proliferation. It is a colorimetric assay, in which the reduction of yellow-colored tetrazolium salt (3-(4,5-dimethylthiazol-2-yl)-2,5-diphenyltetrazolium bromide or MTT) to purple-colored formazan crystals as a result of metabolic activity of cells.

For the MTT assay, to the prepared plates, after adding 15 µl of MTT dye to every single well, the plates were put in the incubator. with temperature at 37°C and CO₂ at 5% for 3 hours. Following this, 150 µl of DMSO was introduced as a solubilizing solution and the MTT suspension was eliminated. This was done without disturbing the formazan crystals. The incubation was left to go on for several minutes and the solution in each well was mixed and shaken using a pipette. This led to lysis of the cells and dissolution of the crystals to spread the purple color. This plate was once again wrapped in aluminum foil before the quantification by measuring the absorbance at 500-550 nm using a multi-well spectrophotometer. A darker solution suggests a higher concentration of cells that are metabolically active and viable. The reaction was conducted in three replicates and the average value was determined. The obtained values were analyzed and calculated and subsequently, graphs were plotted.

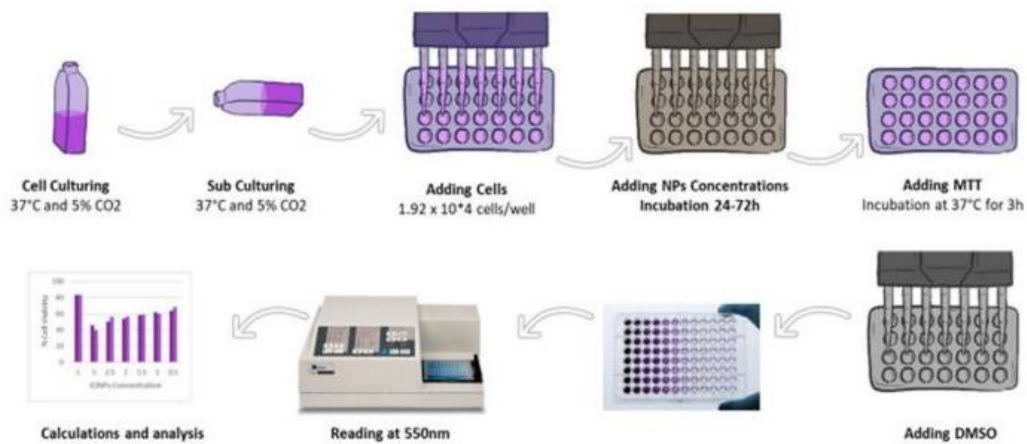


Figure 15: MTT Assay Protocol

Calculation of Cell Survival and Cell Inhibition Percentage

The formula used to evaluate the MTT assay is as follows;

Cell Survival Percentage(%)

$$= \left[\frac{(\text{Absorbance of sample} - \text{Absorbance of Blank})}{\text{Absorbance of Control} - \text{Absorbance of Blank}} \right] \times 100$$

$$\text{Cell Inhibition Percentage } (\%) = 100 - \text{Cell Survival Percentage } (\%)$$

Chapter 04

RESULTS AND DISCUSSIONS

4.1. UV-Visible Spectroscopy

UV-Visible Spectrophotometer Lambda 365 (Perkin Elmer) was used to govern the formation of CDs, and AuCDs. CDs show broad absorption maxima in the ultraviolet (UV) region at 261nm, which is an inherent characteristic peak that corresponds to π - π^* transition of the C=C bonds, in combination with a weak visible range absorption tail. In case of AuCDs, the surface plasmon resonance (SPR) band of Au appeared at 530nm, and the CDs peak broadened (Figure 16). The justification to the broadening is that the intrinsic absorption of the CDs and plasmonic absorption of AuNPs might overlap, leading to a broader absorption profile. For particular applications in sensing, imaging, and photonics, this hybrid absorption behavior can be modified.

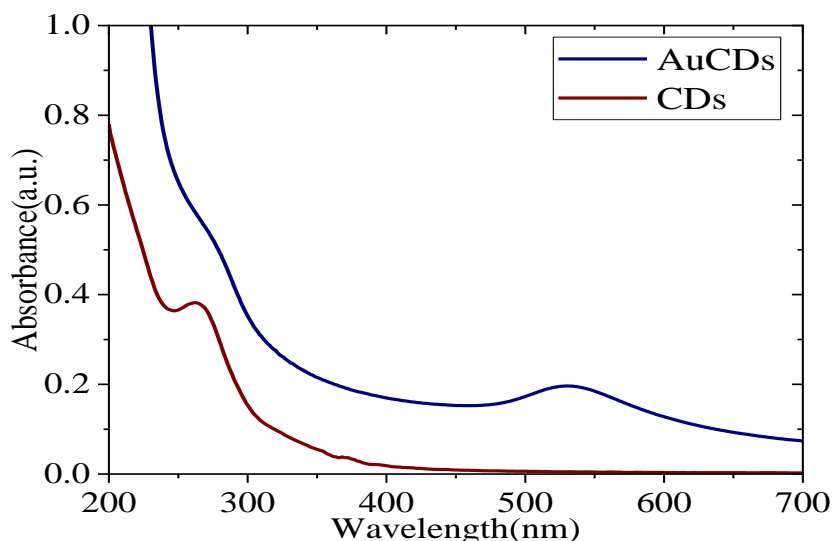


Figure 16: UV-Visible Spectra of Carbon Dots, and AuCDs

4.2. Scanning Electron Microscopy (SEM)

The structure and morphology of CDs, and AuCDs can be confirmed through the scanning electron microscope VEGA3-TESCAN and MIRA3-TESCAN, at an

accelerating voltage of 20 kV and 10kV, respectively. Figure 17 illustrates the SEM image of CDs, and AuCDs. It is obvious that in case of CDs, the nanoparticles are not well dispersed. The average particle diameter of the AuCDs (Figure 17B) core/shell structure was found to be 15 nm.

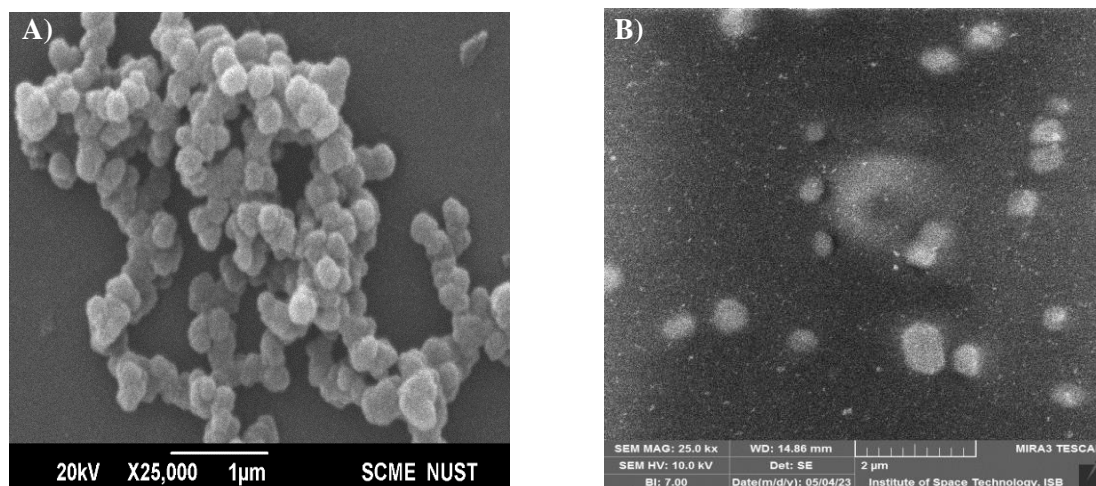
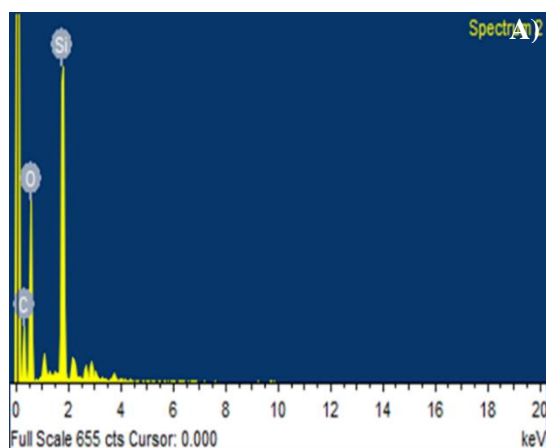


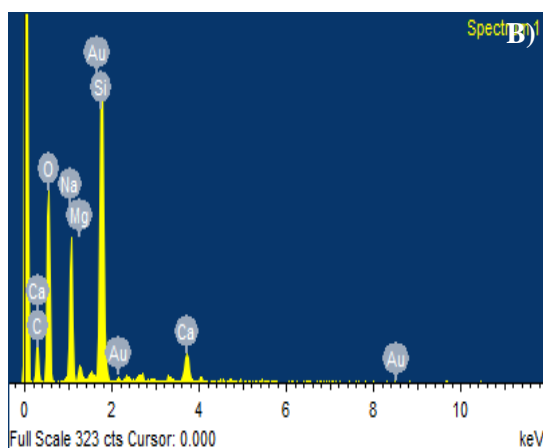
Figure 17: SEM images of core/shell nanoparticles A) Carbon Dots B) AuCDs

4.3. Energy Dispersive X-ray Spectroscopy (EDX)

The elemental composition of CDs, and AuCDs can be confirmed through the elemental analyzer connected with Scanning electron microscope. The successful development of AuCDs is indicated by the presence of Au element in the corresponding elemental table.



Element	Weight %	Atomic %
C K	29.71	38.88
O K	51.56	50.65
Si K	18.72	10.48
Totals	100.00	



Element	Weight%	Atomic%
C K	21.63	30.70
O K	45.52	48.50
Na K	11.55	8.56
Mg K	0.93	0.65
Si K	17.17	10.42
Ca K	2.61	1.11
Au M	0.58	0.0
Totals	100.00	

Figure 18: EDS Spectra and corresponding Elemental Composition of A) Carbon Dots B) AuCDs

4.4. X-Ray Diffraction

XRD patterns were verified through Bruker XRD diffractometer D8 Advance Germany with $\text{CuK}\alpha$ X-ray source. When compared to the XRD pattern of CDs, which exhibits a broad (002) peak at $21.7^\circ(2\theta)$ along with another sharp peak (002) at $28^\circ(2\theta)$ corresponding to graphitic core of CDs, and another small (100) peak at $42^\circ(2\theta)$. It was found that the CDs in the Au-coated CDs were hardly distinguishable. This shows that The CDs' interlayer spacing has increased as a result of AuNPs generation on their surface. (Alarfaj, El-Tohamy, & Oraby, 2018). Additionally, the AuCD's XRD pattern showed the presence of a considerably distinct peak at $45.5^\circ(2\theta)$, demonstrating the distribution of Au (200) on the surface of the CDs.

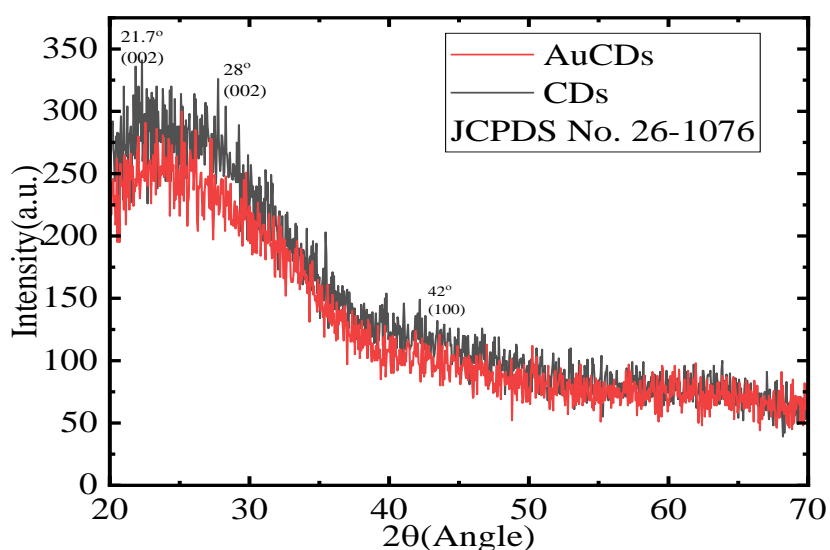


Figure 19: XRD Pattern of Carbon Dots and AuCDs

4.5. Fourier Transform Infrared Spectroscopy

FTIR spectroscopy of the CDs and AuCDs was performed through Bruker Alpha platinum-ATR. The FTIR spectra show a prominent peak at 3434.2 cm^{-1} , which corresponds to the symmetrical and asymmetrical stretch of -OH and N-H. Hydrogen bonding is the cause of the peak's broadening. The peaks at 1634 and 1409 cm^{-1} are correlated with the functional group -COOH. It is anticipated that the aromatic out-of-plane C-H bending peaks at 675.5 cm^{-1} (Figure 20). It is important to note that the capability of donating electrons during the AuCDs formation reaction was demonstrated by the -OH groups' presence and reducing activity on the CDs' surface. Additionally, the high-affinity COOH groups on the surface of CDs for Au ions stimulate Au ion adsorption on the CDs surface and inhibit Au ion aggregation. Thus, in the production of Au coated CDs, CDs can be utilized as stabilization and reduction agents (Alarfaj et al., 2018).

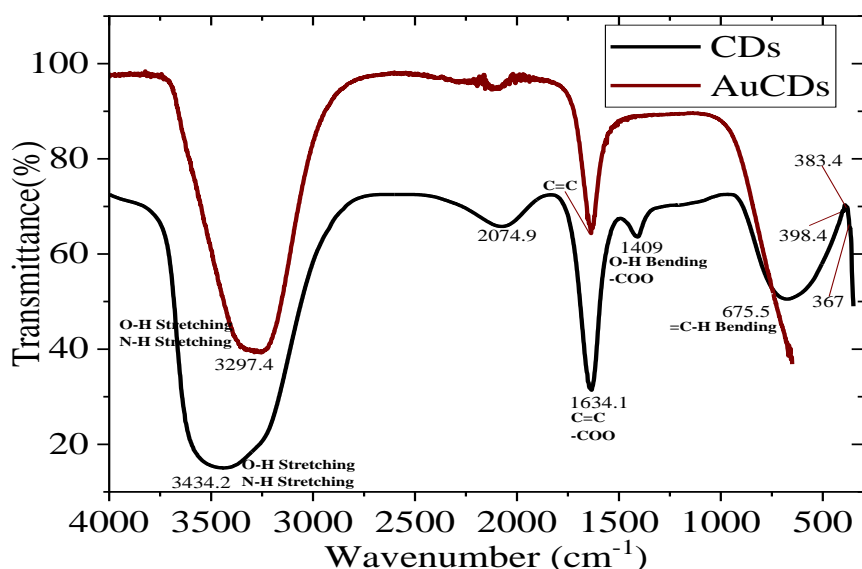


Figure 20: FTIR Spectra of Carbon Dots and AuCDs

4.6. Electrochemical Measurements

A three-electrode Gammy workstation was used to conduct the electrochemical measurements. Without the use of a binder, the functional electrode was prepared by altering a GCE electrode via already prepared NPs. The counter electrode was made of platinum wire. As a reference electrode, an Ag/AgCl system was used. At a scan rate of 20 mV/s and a potential range of 0-2 V, CV measurements were carried out using 0.1M NaOH as an electrolyte. A concentration range of 2-100 mM was used for glucose detection. At room temperature, every measurement was taken. To ensure the reliability and reproducibility of the analysis, every measurement was carried out at least twice.

Glucose Detection Via Electrochemical Sensing

CV was employed for the detection of Glucose. Due to the electrons' relatively easy transit over the phase boundary, the bare nanoparticles CDs and AuCDs showed the highest peaks in the CV tests. The peaks show that the NP-coated electrode surface has a lot of cavities that are open to glucose binding. The glucose molecules linked to the NPs significantly decreased the current signal. This drop in the current signal was inversely correlated with the glucose concentration because glucose obstructs the cavities, making it difficult for redox markers to reach the electrode. These tests verified the CDs and AuCDs sensor's strong sensitivity to glucose. Due to the ultrahigh

sensitivity made possible by the integration of CDs and AuCDs into the sensor composition, the sensor can detect glucose concentrations as low as 2mM (Buk & Pemble, 2019).

Due to their peculiar electrochemical characteristics and surface functionalization capabilities, CDs exhibit significant potential for glucose detection by cyclic voltammetry (CV). The modified electrode with CDs will exhibit peaks in the current-potential curve due to the redox reactions associated with oxidation and the reduction of reaction products. Glucose molecules in the sample solution are oxidized, which generates gluconic acid and hydrogen peroxide H_2O_2 . The generated hydrogen peroxide is then detected through its electrochemical reduction, resulting in a current response. The obtained cyclic voltammogram will show characteristic peaks related to the electrochemical processes of glucose oxidation and reduction of reaction products. Using CDs in cyclic voltammetry for glucose detection offers advantages of enhanced sensitivity, selectivity, and potential for real-time monitoring.

Au-coated Carbon dots have a large surface area, enhancing the reactivity and sensitivity of the electrochemical process. Exceptional electrical conductivity along with catalytic characteristics are provided by the combination of CDs with AuNPs. Functionalization options allow tailoring the sensor for specific analytes, making it highly selective.

CDs exhibit a strong oxidation peak with maximum peak current 0.8mA at voltage 1.7V. The peak shifted from 1.7V to 1.6V on addition of 2mM Glucose and further shifted to 1.4V on addition of 10mM Glucose with substantial decrease in current and almost disappeared into a plateau at 40mM concentration of Glucose. Two additional peaks appeared, one at 1.9V on addition of Glucose which is distinct for all concentrations, and the second started to appear at 20mM concentration of Glucose at voltage 1.05V (Figure 21A).

AuCDs exhibit a strong oxidation peak with maximum peak current 1.1mA at voltage 1.75V. The peak shifted from 1.75V to 1.68V on addition of 2mM Glucose and further shifted to 1.43V on addition of 10mM Glucose with substantial decrease in current and almost disappeared into a plateau at 40mM concentration of Glucose. An additional peak started to appear at 20mM concentration of Glucose at voltage 1.03V (Figure 21B).

Due to their exceptional electrical conductivity and enhanced reactivity and sensitivity to the electrochemical process in contrast to CDs, AuCDs exhibit an elevated amount of current than CDs.

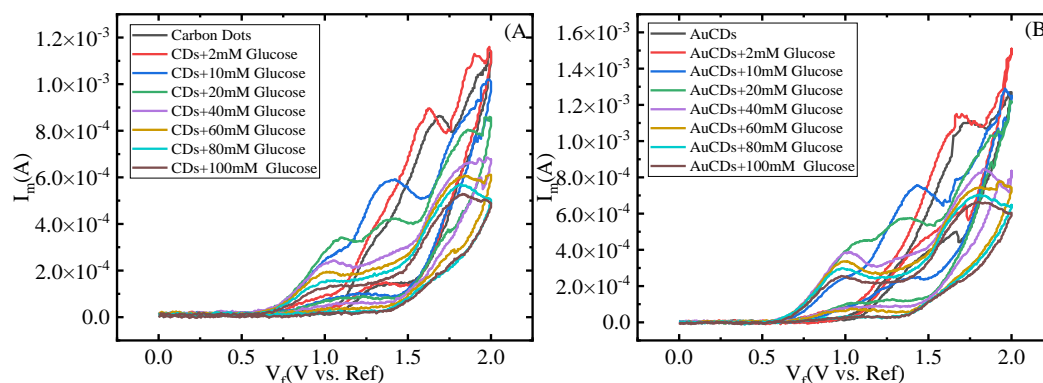


Figure 21: Electrochemical Sensing of Glucose using 0.1M NaOH as electrolyte through A) Carbon Dots B) AuCDs

4.7. Optical Detection of Metal Ions

At a concentration of 0.25 mM, aqueous solutions of metal ions were prepared by dissolving the subsequent salts in deionized water. At room temperature, 0.5 mL of metal salt solutions and 2 mL of NPs solution are mixed together. In case of CDs, the absorbance was observed at three discrete pH values i.e., pH 3, 5, and 8. While, in case of AuCDs the absorbance was observed only at pH value of 5. With the use of a UV-Visible Spectrophotometer, the absorbance intensity and spectrum were captured.

Coordination with metal ions takes place owing to CDs' surface oxygen moieties, which in turn causes the PL to quench, making them suitable for selective and sensitive colorimetric and fluorometric metal ion detection (Bogireddy, Lara, Fragoso, & Agarwal, 2020). PL quenching is primarily caused by the energy transfer between the nano carbons and metal ions via specific chemical reactions caused by surface traps and functionalities.

CDs feature groups on their surface that contain oxygen, such as -OH, -COOH, -OR, C=O, etc. Then, dopants are deposited on the surface of the doped CDs that have groups like -NH₂, -NO₂, -CN, -SH, and -SOH groups. Such species are able to identify a particular metal ion by donating their lone pair of electrons to the metal ion in order to form a coordination complex (Batool et al., 2022).

Particle aggregation and size-dependent optical properties are the basis of the colorimetric AuNP sensor. Colorimetric sensors detect changes in color and the peak of SPR absorbance, which can be attributed to one of two phenomena: (a) metal-induced particle aggregation, or (b) the disintegration of aggregated particles. When functionalized AuNP binds to the target metal ion, it causes metal-induced particle aggregation. This aggregation results in a visible color shift in the assay solution, a red shift, and a broadening of the SPR peak. In the second case, colorimetric sensing is based on the disaggregation of aggregated AuNP probes. The target metal reacts with the aggregated particles to cause disaggregation. As a result, the color changes and the SPR absorption peak blue shifts (Priyadarshini & Pradhan, 2017).

In case of CDs, the CDs peak almost disappeared to a plateau at pH 3 and 8. Absorbance intensity reduced on integration of metal ions with CDs at pH 3. Absorbance intensity varied on integration of metal ions with CDs at pH 8, it reduced with some metal ions and got enhanced with others. Absorbance intensity enhanced on integration of metal ions with CDs at pH 5. In case of Cu, the CDs peak shifted from 260nm to 250nm due to **Coordination Complex Formation** with $-NH_2$ moieties demonstrating, in comparison to other metal ions, a higher selectivity towards Cu ions.

In case of AuCDs, the absorbance intensity enhanced on integration with metal ions but with slight change as compared to CDs where intensity enhanced notably. SPR peak enhanced on integration of Ag, Fe and Cr ions, more notably by Ag ions. CDs plateau enhanced by integration of Fe, Cr, Ag and Cu ions. There is almost no effect in absorption in the case of Sr, Ca, and Ba. There is a minute effect in case of Ni, Li, Co, and Ce.

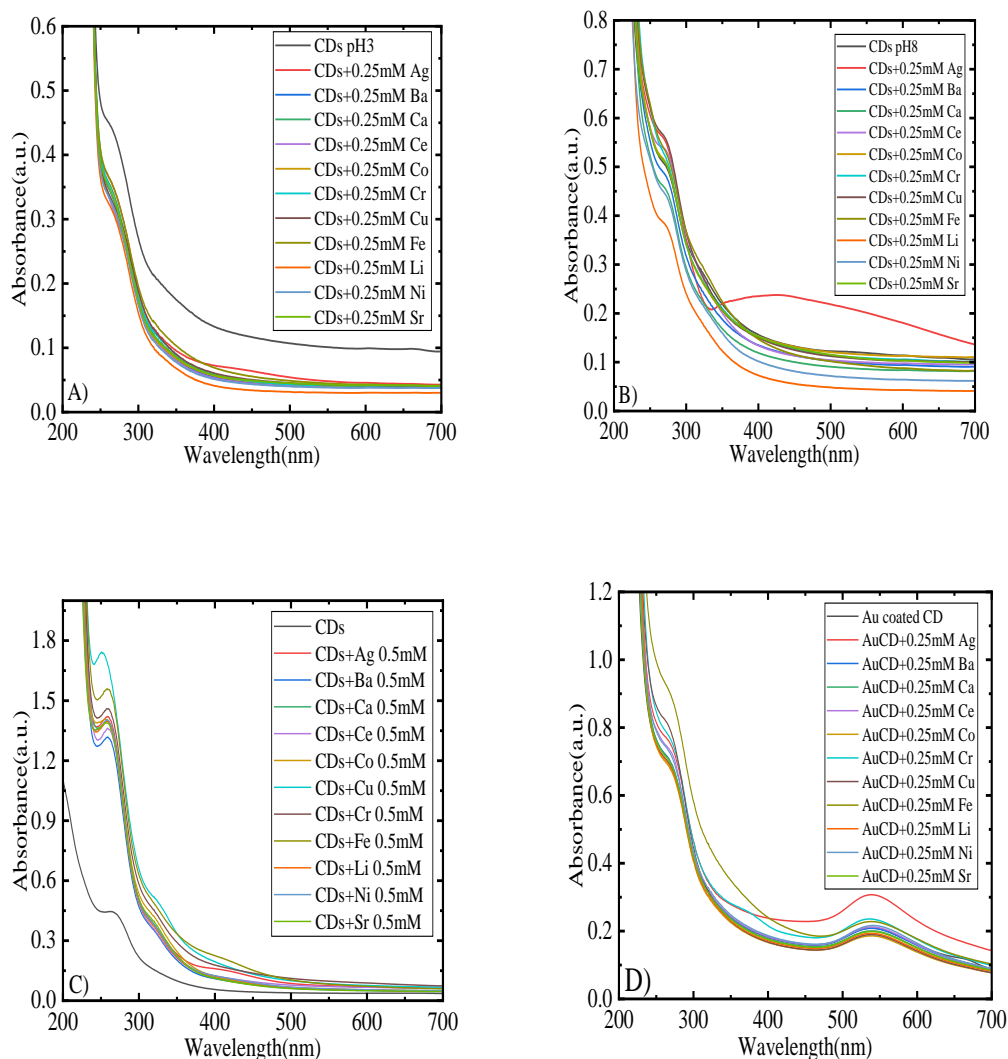


Figure 22: Optical Detection of Metal Ions Via A) CDs at pH3 B) CDs at pH8 C) CDs at pH5 D) AuCDs at pH5

4.8. Cytotoxicity Assessment

For 48 hours, CDs and AuCDs were incubated separately with cancer cells (MDA-MB-231) and normal cells (HEK-293T). Cell viability was tested by MTT assay.

CDs exhibited efficient cell viability against cancer cells MDA-MB-231 (38 % to 90 %) with varying concentration from 250–3.9 μM (Figure 23). Under similar experimental conditions, the cell viability of CDs was significantly higher against normal cell HEK-293T (61 % to 94 %) in comparison to that of cancer cells (Figure 23).

Notably, CDs are more effective at killing cancer cells (MDA-MB-231) than normal cells (HEK-293T) selectively. Reactive oxygen species (ROS) can be generated by CDs

in cells. High ROS concentrations can cause oxidative stress, which harms cellular components and structures and eventually results in cell death. The cytotoxicity of CDs depends primarily on their overall biocompatibility, which is impacted by their surface modifications, composition, and other factors.

Against MDA-MB-231 cancer cells, AuCDs demonstrated effective cell viability ranging from 36% to 63% at multiple concentrations between 250 and 3.9 μ M (Figure 23). The cell viability of AuCDs was substantially higher than that of cancer cells under similar experimental conditions, spanning from 46% to 73% against the normal cell HEK-293T (Figure 23).

The cytotoxicity of AuNPs can also be ascribed to the coating of Au on Carbon dots. In comparison to normal cell lines, MDA cells may experience higher degrees of oxidative stress due to the presence of Au-coated Carbon dots. Reactive oxygen species (ROS) have the ability to trigger apoptosis and cause cellular damage. The synergistic effects of CDs and Au coating may increase cell cytotoxicity. The distinct characteristics of both components may collaborate in an approach that is more toxic to cancerous cells than to healthy cells.

It is obvious that with an increase in concentrations the cell viability decreases, which shows that the cytotoxicity of CDs and AuCDs could rise at higher concentrations but at low concentrations, they were almost not toxic. Also, AuCDs exhibit less cell viability than CDs which means that AuCDs depict higher toxicity than CDs.

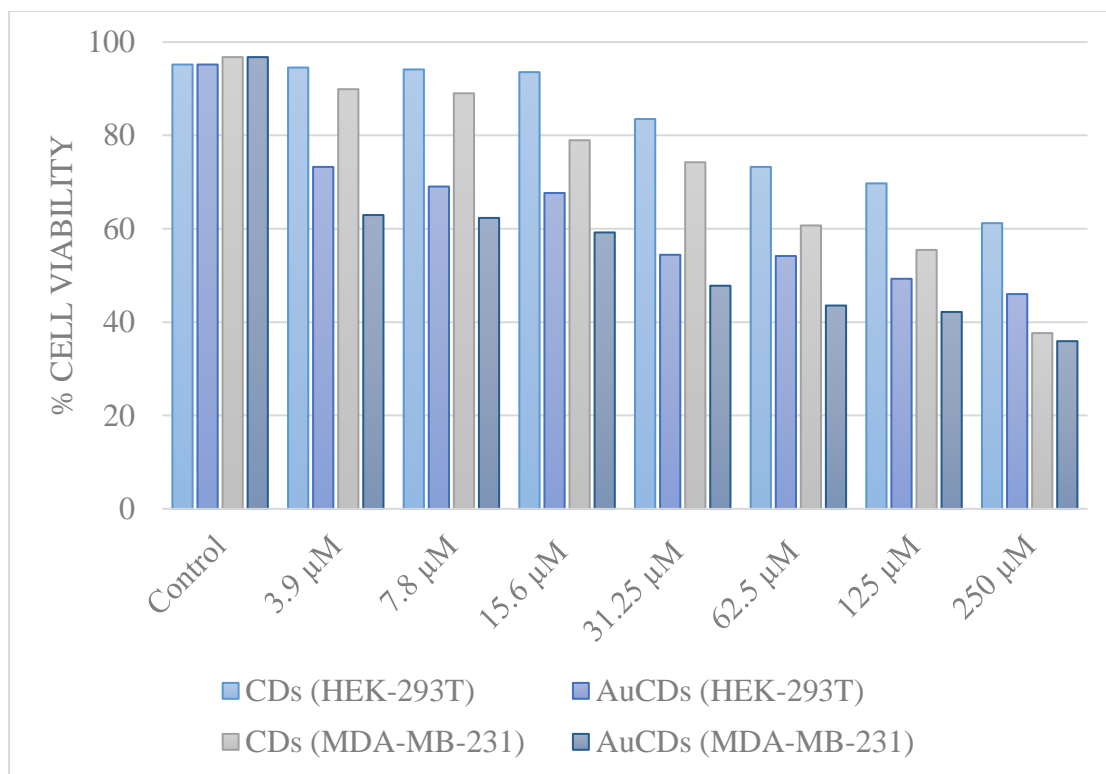


Figure 23: Cytotoxicity Assessment on HEK-293T and MDA-MB-231 Cell Lines via Carbon Dots and AuCDs

Chapter 5

CONCLUSION AND FUTURE RECOMMENDATIONS

In this research, the synthesis protocol of Carbon Dots has been optimized by addition of EDTA to enhance Fluorescence and by addition of additional filtration process to obtain uniform-sized nanoparticles. Further, the Au has been on the surface of Carbon Dots to enhance the Optical, Electrochemical and Biomedical properties of Carbon dots, augmenting their use for versatile applications. The Au coating on Carbon dots is a novelty in this research work and thus, the applications of Au-coated Carbon dots in Electrochemical biosensing of Glucose, Optical detection of metal ions and Cytotoxicity assessment on HEK-293T and MDA-MB-231 cell lines. The structural properties have been studied through XRD, and FTIR; optical properties through UV-Visible spectroscopy, and Fluorescence spectroscopy; morphology through SEM; and elemental composition by EDX.

For Electrochemical biosensing of Glucose, NaOH has been used as electrolyte. Electrode is prepared by Drop cast method on the surface of Glassy Carbon electrode (GCE). Au-coated Carbon dots exhibit exceptional electrical conductivity, enhanced sensitivity, reactivity, and catalytic activity towards Electrochemical biosensing of Glucose as compared to Carbon dots. Electrochemical analysis has been performed using 0.1MNaOH as electrolyte, Platinum wire as counter electrode, and Ag/AgCl as reference electrode.

Optical detection of metal ions has been performed at pH 3, 5, and 8 in case of Carbon dots; and at pH 5 in case of Au-coated Carbon dot. At pH 3 and 8, the Carbon dots peak almost disappeared to a plateau. Using Carbon dots, Cu ions show a blue peak shift from 260nm to 250nm along with the enhancement of intensity. Au-coated Carbon dots also show enhancement on integration with metal ions. Thus, Carbon dots can be utilized as an Optical sensor for metal ion detection.

Cytotoxicity assessment has been performed on HEK-293T (Kidney cells) and MDA-MB-231 (Breast cancer cells). The cytotoxicity of Carbon dots and Au-coated Carbon dots escalated at higher concentrations but at low concentrations, they were almost not toxic. Au-coated Carbon dots display higher cytotoxicity than Carbon dots.

Future Recommendations

In future, Carbon dots and Au-coated Carbon dots can be studied for

- ❖ Electrochemical sensing of various nutrients such as Ascorbic acid, and H₂O₂
- ❖ Fluorometric detection of metal ions
- ❖ Antioxidant activity using DPPH
- ❖ Anti-bacterial activity
- ❖ Cancer therapy

REFERENCES

- 80004-2.; I. O. f. S. J. I. T. (2015). Nanotechnologies—Vocabulary—Part 2: Nano-Objects.
- Alarfaj, N., El-Tohamy, M., & Oraby, H. (2018). CA 19-9 Pancreatic Tumor Marker Fluorescence Immunosensing Detection via Immobilized Carbon Quantum Dots Conjugated Gold Nanocomposite. *International Journal of Molecular Sciences*, *19*, 1162. doi:10.3390/ijms19041162
- Alim, S., Vejayan, J., Yusoff, M. M., & Kafi, A. (2018). Recent uses of carbon nanotubes & gold nanoparticles in electrochemistry with application in biosensing: A review. *Biosensors and Bioelectronics*, *121*, 125-136.
- Ananthapadmanaban, D. (2018). Summary of some selected characterization methods of geopolymers. *Geopolymers and Other Geosynthetics*: IntechOpen.
- Anik, M., Mahmud, N., Masud, A. A., & Hasan, M. (2021). Gold nanoparticles (GNPs) in biomedical and clinical applications: A review. *Nano Select*, *3*. doi:10.1002/nano.202100255
- Antonii, F. J. H. E. B. F. Panacea aurea-auro potabile. *1618*, 250.
- Asha, A. B., & Narain, R. (2020). Nanomaterials properties. *Polymer science and nanotechnology* (pp. 343-359): Elsevier.
- Baker, S. N., & Baker, G. A. (2010). Luminescent carbon nanodots: emergent nanolights. *Angewandte Chemie International Edition*, *49*(38), 6726-6744.
- Bansal, S. A., Kumar, V., Karimi, J., Singh, A. P., & Kumar, S. (2020). Role of gold nanoparticles in advanced biomedical applications. *Nanoscale Advances*, *2*(9), 3764-3787.
- Batool, M., Junaid, H. M., Tabassum, S., Kanwal, F., Abid, K., Fatima, Z., & Shah, A. T. (2022). Metal ion detection by carbon dots—a review. *Critical Reviews in Analytical Chemistry*, *52*(4), 756-767.
- Bogireddy, N. K. R., Lara, J., Fragoso, L. R., & Agarwal, V. (2020). One-step hydrothermal preparation of highly stable N doped oxidized carbon dots for toxic organic pollutants sensing and bioimaging. *Chemical Engineering Journal*, *401*, 126097. doi:<https://doi.org/10.1016/j.cej.2020.126097>
- Buk, V., & Pemble, M. E. (2019). A highly sensitive glucose biosensor based on a micro disk array electrode design modified with carbon quantum dots and gold

- nanoparticles. *Electrochimica Acta*, 298, 97-105.
doi:<https://doi.org/10.1016/j.electacta.2018.12.068>
- Buk, V., Pemble, M. E., & Twomey, K. (2019). Fabrication and evaluation of a carbon quantum dot/gold nanoparticle nanohybrid material integrated onto planar micro gold electrodes for potential bioelectrochemical sensing applications. *Electrochimica Acta*, 293, 307-317.
doi:<https://doi.org/10.1016/j.electacta.2018.10.038>
- Campuzano, S., Yáñez-Sedeño, P., & Pingarrón, J. M. (2019). Carbon dots and graphene quantum dots in electrochemical biosensing. *Nanomaterials*, 9(4), 634.
- Chang, G., Shu, H., Ji, K., Oyama, M., Liu, X., & He, Y. (2014). Gold nanoparticles directly modified glassy carbon electrode for non-enzymatic detection of glucose. *Applied Surface Science*, 288, 524-529.
doi:<https://doi.org/10.1016/j.apsusc.2013.10.064>
- Chao-Mujica, F., Garcia-Hernández, L., Camacho-López, S., Camacho-López, M., Camacho-López, M., Reyes Contreras, D., . . . Darias-Gonzalez, J. (2021). Carbon quantum dots by submerged arc discharge in water: Synthesis, characterization, and mechanism of formation. *Journal of Applied Physics*, 129(16).
- Cho, I.-H., Kim, D. H., & Park, S. (2020). Electrochemical biosensors: perspective on functional nanomaterials for on-site analysis. *Biomaterials Research*, 24(1), 6.
doi:10.1186/s40824-019-0181-y
- Chowdhury, M., Pal, S., Ghosh, A., & Kumar Das, P. (2023). Co²⁺ Doped Biotinylated Carbon Dot: A Theranostic Agent for Target Specific Killing of Cancer Cells via Hypoxia Induced Apoptosis. *Chemistry–A European Journal*, 29(37), e202300928.
- Das, R. K., & Mohapatra, S. (2017). Highly luminescent, heteroatom-doped carbon quantum dots for ultrasensitive sensing of glucosamine and targeted imaging of liver cancer cells. *Journal of Materials Chemistry B*, 5(11), 2190-2197.
- De, B., & Karak, N. (2017). Recent progress in carbon dot–metal based nanohybrids for photochemical and electrochemical applications. *Journal of Materials Chemistry A*, 5(5), 1826-1859.

- Deng, J., Lu, Q., Mi, N., Li, H., Liu, M., Xu, M., . . . Yao, S. (2014). Electrochemical synthesis of carbon nanodots directly from alcohols. *Chemistry—A European Journal*, 20(17), 4993-4999.
- Despotopoulou, M. (2019). Characterisations of Co₃O₄ thin films deposited by DLI-MOCVD for the photoelectrocatalysis of water.
- Ding, C., Zhu, A., & Tian, Y. (2014). Functional surface engineering of C-dots for fluorescent biosensing and in vivo bioimaging. *Accounts of chemical research*, 47(1), 20-30.
- Ding, Y., Zhang, F., Xu, J., Miao, Y., Yang, Y., Liu, X., & Xu, B. (2017). Synthesis of short-chain passivated carbon quantum dots as the light emitting layer towards electroluminescence. *RSC Advances*, 7(46), 28754-28762. doi:10.1039/C7RA02421E
- Dorđević, L., Arcudi, F., Cacioppo, M., & Prato, M. (2022). A multifunctional chemical toolbox to engineer carbon dots for biomedical and energy applications. *Nature Nanotechnology*, 17(2), 112-130. doi:10.1038/s41565-021-01051-7
- Ezzahmouly, M., Elmoutaouakkil, A., Ed-Dhahraouy, M., Hamza, K., Elouahli, A., Mazurier, A., . . . Hatim, Z. (2019). Micro-computed tomographic and SEM study of porous bioceramics using an adaptive method based on the mathematical morphological operations. *Heliyon*, 5, e02557. doi:10.1016/j.heliyon.2019.e02557
- Faraday, M. (1996). Experimental relations of gold (and other metals) to light. *SPIE MILESTONE SERIES MS, 120*, 9-27.
- Faulk, W. P., & Taylor, G. M. (1971). Communication to the editors: an immunocolloid method for the electron microscope. *Immunochemistry*, 8(11), 1081-1083.
- Feynman, R. P. (1960). An invitation to enter a new field of physics. *Int. J. Eng. Sci*, 23(8).
- Gao, G., Jiang, Y.-W., Jia, H.-R., Yang, J., & Wu, F.-G. (2018). On-off-on fluorescent nanosensor for Fe³⁺ detection and cancer/normal cell differentiation via silicon-doped carbon quantum dots. *Carbon*, 134, 232-243.
- Gayen, B., Palchoudhury, S., & Chowdhury, J. (2019). Carbon dots: A mystic star in the world of nanoscience. *Journal of Nanomaterials*, 2019, 1-19.
- Hameed, M. K., Ahmady, I. M., Alawadhi, H., Workie, B., Sahle-Demessie, E., Han, C., . . . Mohamed, A. A. (2018). Gold-carbon nanoparticles mediated delivery

- of BSA: Remarkable robustness and hemocompatibility. *Colloids and Surfaces A: Physicochemical and Engineering Aspects*, 558, 351-358.
- Jeyarani, S., Vinita, N. M., Puja, P., Senthamilselvi, S., Devan, U., Velangani, A. J., . . . Kumar, P. (2020). Biomimetic gold nanoparticles for its cytotoxicity and biocompatibility evidenced by fluorescence-based assays in cancer (MDA-MB-231) and non-cancerous (HEK-293) cells. *Journal of Photochemistry and Photobiology B: Biology*, 202, 111715.
- Ji, H., Zhou, F., Gu, J., Shu, C., Xi, K., & Jia, X. (2016). Nitrogen-doped carbon dots as a new substrate for sensitive glucose determination. *Sensors*, 16(5), 630.
- Jorns, M., & Pappas, D. (2021). A review of fluorescent carbon dots, their synthesis, physical and chemical characteristics, and applications. *Nanomaterials*, 11(6), 1448.
- Khairol Anuar, N. K., Tan, H. L., Lim, Y. P., So'aib, M. S., & Abu Bakar, N. F. (2021). A review on multifunctional carbon-dots synthesized from biomass waste: Design/fabrication, characterization and applications. *Frontiers in Energy Research*, 9, 67.
- Khan, I., Saeed, K., & Khan, I. (2019). Nanoparticles: Properties, applications and toxicities. *Arabian journal of chemistry*, 12(7), 908-931.
- Kothleitner, G., Neish, M. J., Lugg, N. R., Findlay, S., Grogger, W., Hofer, F., & Allen, L. J. (2014). Quantitative elemental mapping at atomic resolution using X-ray spectroscopy. *Physical Review Letters*, 112(8), 085501.
- Lee, J.-S. (2010). Recent progress in gold nanoparticle-based non-volatile memory devices. *Gold Bulletin*, 43(3), 189-199. doi:10.1007/BF03214986
- Lee, Y. J., Ahn, E.-Y., & Park, Y. (2019). Shape-dependent cytotoxicity and cellular uptake of gold nanoparticles synthesized using green tea extract. *Nanoscale Research Letters*, 14, 1-14.
- Li, X., Shi, L., Li, L., Dong, C., Li, C.-z., & Shuang, S. (2019). Recent advances in carbon nanodots: properties and applications in cancer diagnosis and treatment. *Journal of Analysis and Testing*, 3, 37-49.
- Liu, J., Li, R., & Yang, B. (2020). Carbon dots: A new type of carbon-based nanomaterial with wide applications. *ACS Central Science*, 6(12), 2179-2195.

- Liu, Y., Hardie, J., Zhang, X., & Rotello, V. M. (2017, December). Effects of engineered nanoparticles on the innate immune system. *Seminars in immunology*, Vol. 34, 25-32. Academic Press.
- Lo, C. K., Xiao, D., & Choi, M. M. (2007). Homocysteine-protected gold-coated magnetic nanoparticles: synthesis and characterisation. *Journal of Materials Chemistry*, 17(23), 2418-2427.
- Long, J., Nand, A., & Ray, S. (2021). Application of spectroscopy in additive manufacturing. *Materials*, 14(1), 203.
- Mehranfar, A., & Izadyar, M. (2020). Theoretical design of functionalized gold nanoparticles as antiviral agents against severe acute respiratory syndrome coronavirus 2 (SARS-CoV-2). *The Journal of Physical Chemistry Letters*, 11(24), 10284-10289.
- Mihalache, I., Radoi, A., Mihaila, M., Munteanu, C., Marin, A., Danila, M., . . . Kusko, C. (2015). Charge and energy transfer interplay in hybrid sensitized solar cells mediated by graphene quantum dots. *Electrochimica Acta*, 153, 306-315. doi:<https://doi.org/10.1016/j.electacta.2014.11.200>
- Na, N., Liu, T., Xu, S., Zhang, Y., He, D., Huang, L., & Ouyang, J. (2013). Application of fluorescent carbon nanodots in fluorescence imaging of human serum proteins. *Journal of Materials Chemistry B*, 1(6), 787-792.
- Nguyen, V., Yan, L., Xu, H., & Yue, M. (2018). One-step synthesis of multi-emission carbon nanodots for ratiometric temperature sensing. *Applied Surface Science*, 427, 1118-1123. doi:<https://doi.org/10.1016/j.apsusc.2017.08.133>
- Örenli, D., Kaçar Selvi, C., Öztürk, F., Erden, P. E., & Kılıç, E. (2023). Electrochemical (bio)sensors based on carbon quantum dots, ionic liquid and gold nanoparticles for bisphenol A. *Analytical Biochemistry*, 662, 115002. doi:<https://doi.org/10.1016/j.ab.2022.115002>
- Ortega-Liebana, M. C., Encabo-Berzosa, M. M., Ruedas-Rama, M. J., & Hueso, J. L. (2017). Nitrogen-Induced Transformation of Vitamin C into Multifunctional Up-converting Carbon Nanodots in the Visible–NIR Range. *Chemistry–A European Journal*, 23(13), 3067-3073.
- Papaioannou, N., Titirici, M.-M., & Sapelkin, A. (2019). Investigating the effect of reaction time on carbon dot formation, structure, and optical properties. *ACS omega*, 4(26), 21658-21665.

- Patil, T., Gambhir, R., Vibhute, A., & Tiwari, A. P. (2023). Gold Nanoparticles: Synthesis Methods, Functionalization and Biological Applications. *Journal of Cluster Science*, 34(2), 705-725. doi:10.1007/s10876-022-02287-6
- Pingarrón, J. M., Yáñez-Sedeño, P., & González-Cortés, A. (2008). Gold nanoparticle-based electrochemical biosensors. *Electrochimica Acta*, 53(19), 5848-5866. doi:<https://doi.org/10.1016/j.electacta.2008.03.005>
- Priyadarshini, E., & Pradhan, N. (2017). Gold nanoparticles as efficient sensors in colorimetric detection of toxic metal ions: A review. *Sensors and Actuators B: Chemical*, 238, 888-902. doi:<https://doi.org/10.1016/j.snb.2016.06.081>
- Rahi, S. K., Hassan, E. S., & Abd, A. N. (2016). Spectroscopic methods studies in polymer. *World Scientific News*, (42), 41-53.
- Rocha, F. S., Gomes, A. J., Lunardi, C. N., Kaliaguine, S., & Patience, G. S. (2018). Experimental methods in chemical engineering: Ultraviolet visible spectroscopy—UV-Vis. *The Canadian Journal of Chemical Engineering*, 96(12), 2512-2517. doi:<https://doi.org/10.1002/cjce.23344>
- Romero, M. P., Alves, F., Stringasci, M. D., Buzzá, H. H., Ciol, H., Inada, N. M., & Bagnato, V. S. (2021). One-pot microwave-assisted synthesis of carbon dots and in vivo and in vitro antimicrobial photodynamic applications. *Frontiers in Microbiology*, 12, 662149.
- Sachdev, A., & Gopinath, P. (2015). Green synthesis of multifunctional carbon dots from coriander leaves and their potential application as antioxidants, sensors and bioimaging agents. *Analyst*, 140(12), 4260-4269.
- Sadiq, Z., Safiabadi Tali, S. H., Hajimiri, H., Al-Kassawneh, M., & Jahanshahi-Anbuhi, S. Gold Nanoparticles-Based Colorimetric Assays for Environmental Monitoring and Food Safety Evaluation. *Critical Reviews in Analytical Chemistry*, 1-36. doi:10.1080/10408347.2022.2162331
- Salem, S. S., Hammad, E. N., Mohamed, A. A., & El-Dougdoug, W. (2022). A comprehensive review of nanomaterials: Types, synthesis, characterization, and applications. *Biointerface Res. Appl. Chem*, 13(1), 41.
- Sangeetha, V. P., Smriti, S., Solanki, P. R., & Mohanan, P. V. (2021). Mechanism of action and cellular responses of HEK293 cells on challenge with zwitterionic carbon dots. *Colloids and Surfaces B: Biointerfaces*, 202, 111698. doi:<https://doi.org/10.1016/j.colsurfb.2021.111698>

- Sani, A., Cao, C., & Cui, D. (2021). Toxicity of gold nanoparticles (AuNPs): A review. *Biochemistry and Biophysics Reports*, 26, 100991.
- Silva, F., Cabral Campello, M. P., & Paulo, A. (2020). Radiolabeled Gold Nanoparticles for Imaging and Therapy of Cancer. *Materials*, 14(1), 4.
- Sivasankarapillai, V. S., Kirthi, A. V., Akksadha, M., Indu, S., Dharshini, U. D., Pushpamalar, J., & Karthik, L. (2020). Recent advancements in the applications of carbon nanodots: Exploring the rising star of nanotechnology. *Nanoscale Advances*, 2(5), 1760-1773.
- Sonawane, R. S., & Dongare, M. K. (2006). Sol–gel synthesis of Au/TiO₂ thin films for photocatalytic degradation of phenol in sunlight. *Journal of Molecular Catalysis A: Chemical*, 243(1), 68-76. doi:<https://doi.org/10.1016/j.molcata.2005.07.043>
- Sun, Y.-P., Zhou, B., Lin, Y., Wang, W., Fernando, K. S., Pathak, P., . . . Wang, H. (2006). Quantum-sized carbon dots for bright and colorful photoluminescence. *Journal of the American Chemical Society*, 128(24), 7756-7757.
- Taniguchi, N. (1974). On the Basic Concept of 'Nano-technology'. *Proc. Intl. Conf. Prod. Eng. Tokyo, Part II, 1974*. Japan Society of Precision Engineering.
- Teimuri-Mofrad, R., Hadi, R., Tahmasebi, B., Farhoudian, S., Mehravar, M., & Nasiri, R. (2017). Green synthesis of gold nanoparticles using plant extract: Mini-review. *Nanochemistry Research*, 2(1), 8-19.
- Turkevich, J., Stevenson, P. C., & Hillier, J. (1951). A study of the nucleation and growth processes in the synthesis of colloidal gold. *Discussions of the Faraday Society*, 11, 55-75.
- Vemuri, S. K., Banala, R. R., Mukherjee, S., Uppula, P., Subbaiah, G., AV, G. R., & Malarvilli, T. (2019). Novel biosynthesized gold nanoparticles as anti-cancer agents against breast cancer: Synthesis, biological evaluation, molecular modelling studies. *Materials Science and Engineering: C*, 99, 417-429.
- Venkata Sivareddy, D., Krishna, P. V., & Venu Gopal, A. (2022). Effect of thermo-mechanical loading on machining induced residual stresses in ultrasonic vibration assisted turning of Ti6Al4V alloy. *Proceedings of the Institution of Mechanical Engineers, Part B: Journal of Engineering Manufacture*, 236(13), 1793-1806.

- Xu, J., Cui, K., Gong, T., Zhang, J., Zhai, Z., Hou, L., . . . Yuan, C. (2022). Ultrasonic-assisted synthesis of N-doped, multicolor carbon dots toward fluorescent inks, fluorescence sensors, and logic gate operations. *Nanomaterials*, *12*(3), 312.
- Xu, X., Ray, R., Gu, Y., Ploehn, H. J., Gearheart, L., Raker, K., & Scrivens, W. A. (2004). Electrophoretic analysis and purification of fluorescent single-walled carbon nanotube fragments. *Journal of the American Chemical Society*, *126*(40), 12736-12737.
- Yang, S.-T., Wang, X., Wang, H., Lu, F., Luo, P. G., Cao, L., . . . Chen, M. (2009). Carbon dots as nontoxic and high-performance fluorescence imaging agents. *The Journal of Physical Chemistry C*, *113*(42), 18110-18114.
- Yang, X., Yang, M., Pang, B., Vara, M., & Xia, Y. (2015). Gold Nanomaterials at Work in Biomedicine. *Chemical reviews*, *115*(19), 10410-10488.
- Yao, Y.-Y., Gedda, G., Girma, W. M., Yen, C.-L., Ling, Y.-C., & Chang, J.-Y. (2017). Magnetofluorescent Carbon Dots Derived from Crab Shell for Targeted Dual-Modality Bioimaging and Drug Delivery. *ACS Applied Materials & Interfaces*, *9*(16), 13887-13899. doi:10.1021/acsami.7b01599
- Ye, Z., Li, G., Lei, J., Liu, M., Jin, Y., & Li, B. (2020). One-Step and One-Precursor Hydrothermal Synthesis of Carbon Dots with Superior Antibacterial Activity. *ACS Applied Bio Materials*, *3*(10), 7095-7102. doi:10.1021/acsabm.0c00923
- Zhang, Y., Wang, Y., Feng, X., Zhang, F., Yang, Y., & Liu, X. (2016). Effect of reaction temperature on structure and fluorescence properties of nitrogen-doped carbon dots. *Applied Surface Science*, *387*, 1236-1246.
- Zhao, P., Li, N., & Astruc, D. (2013). State of the art in gold nanoparticle synthesis. *Coordination Chemistry Reviews*, *257*(3-4), 638-665.
- Zheng, X., Liu, W., Gai, Q., Tian, Z., & Ren, S. (2019). A carbon-dot-based fluorescent probe for the sensitive and selective detection of Copper (II) Ions. *ChemistrySelect*, *4*(8), 2392-2397.
- Zhu, C., Liang, S., Song, E., Zhou, Y., Wang, W., Shan, F., . . . Zhang, T. (2018). In-situ liquid cell transmission electron microscopy investigation on oriented attachment of gold nanoparticles. *Nature communications*, *9*(1), 421.
- Zou, C. e., Yang, B., Bin, D., Wang, J., Li, S., Yang, P., . . . Du, Y. (2017). Electrochemical synthesis of gold nanoparticles decorated flower-like graphene

for high sensitivity detection of nitrite. *Journal of Colloid and Interface Science*,
488, 135-141.